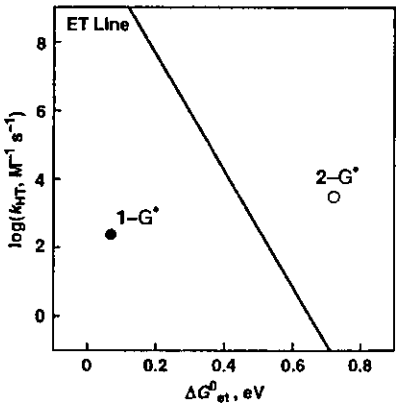

Figure 4. Plot of the rate constant of hydrogen transfer from **1** or **2** to G• ($\log k_{HT}$) vs the free energy of electron transfer from **1** or **2** to G• (ΔG^0_{et}). The solid line shows the dependence of the calculated rate constant of electron transfer (k_{et}) on ΔG^0_{et} based on eq 2, see text.

direct one-step hydrogen atom transfer.[32] In such a case, no effect of Mg^{2+} on the k_{HT} values is observed as shown in Figure 2b (white circles), demonstrating sharp contrast with the case of the electron-transfer reaction from **1** to G•. The k_{HT} value of

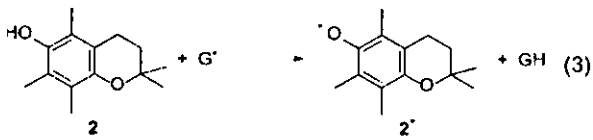

the **2**−G• system is much larger than the estimated k_{et} value as shown in Figure 4 (white circle). This confirms that the hydrogen transfer proceeds via a direct one-step hydrogen atom transfer rather than via electron transfer.

The E_{ox} value of cumylperoxyl radical determined directly by the cyclic voltammetry is located at 0.65 V vs SCE. Thus, the electron transfer from **1** (E_{ox} vs SCE = 0.12 V) to cumylperoxyl radical is energetically feasible ($\Delta G_{et} < 0$). In such a case, the acceleration of the rate of electron transfer from **1** to G• was observed by the presence of metal ions.

In conclusion, the hydrogen transfer from (+)-catechin to galvinoxyl and cumylperoxyl radicals proceeds via electron transfer followed by proton transfer. These results suggest that a hydrogen-transfer reaction from catechins to hydroxyl radical, which is the most powerful reactive oxygen species having a very high reduction potential, proceeds via electron transfer followed by proton transfer.

Acknowledgment. This work was partially supported by a Grant-in-Aid for Scientific Research Priority Area (No. 11228205) from the Ministry of Education, Culture, Sports, Science and Technology, Japan.

References and Notes

(1) Ruch, R. J.; Cheng, S.; Klaunig, J. E. *Carcinogenesis* **1989**, *10*, 1003.
(2) Scoot, B. C.; Butler, J.; Halliwell, B.; Aruoma, O. I. *Free Radical Res. Commun.* **1993**, *19*, 241.
(3) Morei, I.; Lescoat, G.; Cogrei, P.; Sergent, O.; Pasdeloup, N.; Brissot, P.; Cillard, P.; Cillard, J. *Biochem. Pharmacol.* **1993**, *45*, 13.
(4) Hanasaki, Y.; Ogawa, S.; Fukui, S. *Free Radical Biol. Med.* **1994**, *16*, 845.
(5) Zhao, B.; Li, X. J.; He, R. G.; Cheng, S. J.; Xin, W. J. *Cell Biophys.* **1995**, *14*, 9881.
(6) Nanjo, F.; Goto, K.; Seto, R.; Suzuki, M.; Sakai, M.; Hara, Y. *Free Radical Biol. Med.* **1996**, *21*, 895.
(7) Lotito, S. B.; Fraga, C. G. *Free Radical Biol. Med.* **1998**, *24*, 435.
(8) Kashima, M. *Chem. Pharm. Bull.* **1999**, *47*, 279.
(9) Toschi, T. G.; Bordoni, A.; Hrelia, S.; Bendini, A.; Lercker, G.; Biagi, P. L. *J. Agric. Food Chem.* **2000**, *48*, 3973.
(10) Chen, Z. Y.; Chan, P. T.; Ho, K. Y.; Fung, K. P.; Wang, *J. Chem. Phys. Lipids* **1996**, *79*, 157.
(11) Lien, E. J.; Ren, S.; Bui, H.-H.; Wang, R. *Free Radical Biol. Med.* **1999**, *26*, 285.
(12) Wright, J. S.; Johnson, E. R.; DiLabio, G. A. *J. Am. Chem. Soc.* **2001**, *123*, 1173.
(13) Yang, B.; Kotani, A.; Arai, K.; Kusu, F. *Chem. Pharm. Bull.* **2001**, *49*, 747.
(14) Fukuzumi, S.; Tokuda, Y.; Chiba, Y.; Greci, L.; Carloni, P.; Damiani, E. *J. Chem. Soc., Chem. Commun.* **1993**, 1575.
(15) Russell, G. A. *Free Radicals*; Kochi, J. K., Ed.; Willy & Sons: New York, 1973; Chapter 7.
(16) Russell, G. A. *Can. J. Chem.* **1956**, *34*, 1074.
(17) Howard, J. A.; Ingold, K. U.; Symonds, M. *Can. J. Chem.* **1968**, *46*, 1017.
(18) Perrin, D. D.; Armarego, W. L. F.; Perrin, D. R. *Purification of Laboratory Chemicals*; Pergamon Press: Elmsford, NY, 1988.
(19) Fukuhara, K.; Nakanishi, I.; Kansui, H.; Sugiyama, E.; Kimura, M.; Shimada, T.; Urano, S.; Yamaguchi, K.; Miyata, N. *J. Am. Chem. Soc.* **2002**, *124*, 5952.
(20) (a) Nakanishi, I.; Fukuhara, K.; Ohkubo, K.; Shimada, T.; Kansui, H.; Kurihara, M.; Urano, S.; Fukuzumi, S.; Miyata, N. *Chem. Lett.* **2001**, 1152. (b) Sawai, Y.; Sakata, K. *J. Agric. Food Chem.* **1998**, *46*, 111.
(21) Sheldon, R. A. In *The Activation of Dioxygen and Homogeneous Catalytic Oxidation*; Barton, D. H. R., Martell, A. E., Sawyer, D. T., Eds.; Plenum: New York and London, 1933; pp 9−30.
(22) Parshall, G. W.; Ittel, S. D. *Homogeneous Catalysis*, 2nd ed.; Wiley: New York, 1992; Chapter 10.
(23) Sheldon, R.; Kochi, J. K. *Adv. Catal.* **1976**, *25*, 72.
(24) Shilov, A. E. *Activation of Saturated Hydrocarbons by Transition Metal Complexes*; D. Reidel Publishing Co.: Dordrecht, The Netherlands, 1984; Chapter 4.
(25) Bottcher, A.; Birnbaum, E. R.; Day, M. W.; Gray, H. B.; Grinstaff, M. W.; Labinger, J. A. *J. Mol. Catal.* **1997**, *117*, 229.
(26) Kochi, J. K. *Free Radicals in Solution*; J. Wiley & Sons: New York, 1957.
(27) (a) Kochi, J. K.; Krusic, P. J.; Eaton, D. R. *J. Am. Chem. Soc.* **1969**, *91*, 1877. (b) Kochi, J. K.; Krusic, P. J. *J. Am. Chem. Soc.* **1968**, *90*, 7155. (c) Kochi, J. K.; Krusic, P. J. *J. Am. Chem. Soc.* **1969**, *91*, 3938. (d) Kochi, J. K.; Krusic, P. J. *J. Am. Chem. Soc.* **1969**, *91*, 3942. (e) Kochi, J. K.; Krusic, P. J. *J. Am. Chem. Soc.* **1969**, *91*, 3944. (f) Howard, J. A.; Furimsky, E. *Can. J. Chem.* **1974**, *52*, 555.
(28) Fukuzumi, S.; Ono, Y. *J. Chem. Soc., Perkin Trans. 2* **1977**, 622.
(29) Fukuzumi, S.; Ono, Y. *J. Chem. Soc., Perkin Trans. 2* **1977**, 784.
(30) Fukuzumi, S.; Ohkubo, K. *Chem. Eur. J.* **2000**, *6*, 4532.
(31) Itoh, S.; Kumei, H.; Nagatomo, S.; Kitagawa, T.; Fukuzumi, S. *J. Am. Chem. Soc.* **2001**, *123*, 2165.
(32) Nakanishi, I.; Fukuhara, K.; Shimada, T.; Ohkubo, K.; Iizuka, Y.; Inami, K.; Mochizuki, M.; Urano, S.; Itoh, S.; Miyata, N.; Fukuzumi, S. *J. Chem. Soc., Perkin Trans. 2* **2002**, 1520.

J|A|C|S
COMMUNICATIONS

Published on Web 05/07/2002

Enhanced Radical-Scavenging Activity of a Planar Catechin Analogue

Kiyoshi Fukuhara,*,† Ikuo Nakanishi,†,‡ Hisao Kansui,† Etsuko Sugiyama,§ Mitsuhiro Kimura,|| Tomokazu Shimada,|| Shiro Urano,|| Kentaro Yamaguchi,⊥ and Naoki Miyata#

Division of Organic Chemistry, National Institute of Health Sciences, Setagaya-ku, Tokyo 158-8501, Redox Regulation Research Group, National Institute of Radiological Sciences, Japan Science and Technology Corporation (JST), Inage-ku, Chiba 263-8555, Showa Women's University, Setagaya-ku, Tokyo 154-8533, Department of Applied Chemistry, Shibaura Institute of Technology, Minato-ku, Tokyo 108-8548, Chemical Analysis Center, Chiba University, JST, Inage-ku, Chiba 263-8522, and Graduate School of Pharmaceutical Sciences, Nagoya City University, Mizuho-ku, Nagoya 467-8603, Japan

Received December 20, 2001

Oxidative stress is important in the pathogenesis of neuronal cell death in Alzheimer's[1] and Parkinson's[2] disease. The protective role of antioxidants against such pathogens has been widely studied, and this has promoted the development of antioxidants for the treatment of diseases associated with oxidative stress.[3-5] Vitamin E, which is an essential nutrient in humans, may be a clinically useful antioxidant. In fact, α-tocopherol reduces amyloid-induced cell death and suppresses the progression of Alzheimer's disease.[3] Flavonoids such as catechin (**1**) and quercetin (**2**) are plant phenolic pigment products that act as natural antioxidants. Quercetin, on one hand, has been shown to protect against oxidant injury and cell death[6] by scavenging free radicals,[7] protecting against lipid peroxidation,[8] and thereby terminating the chain-radical reaction.[9] On the other hand, there have been only a few reports on the use of catechin for the treatment of free radical-associated disease, whereas the mechanism to scavenge oxygen radical has been well-studied.[10] However, its ability to scavenge free radicals must be improved, and adequate lipophilicity is needed to penetrate the cell membrane before it is suitable for clinical use. The superior antioxidant ability of **2** results from the formation of a stable radical, due to the C2 C3 double bond and the resulting planar geometry which delocalizes the radical throughout the entire molecule.[11] Since the B ring in **1** is known to be perpendicular to the A ring,[12] the radical-scavenging ability of **1** might be improved by constraining the geometry of **1** to be planar. In this communication, we describe the first synthesis and characterization of the antioxidant properties of a planar catechin analogue (**3**) with respect to the chroman and catechol moieties of **1**, by taking advantage of the formation of a bridge between the 3-OH group on ring C and C6′ on ring B.

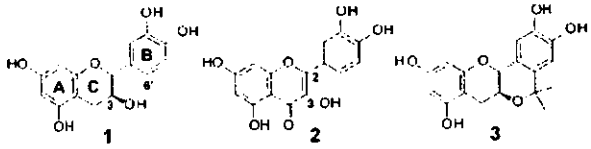

The planar catechin (**3**) was synthesized via an oxa-Pictet Spengler reaction[13] using catechin and acetone with $BF_3{\cdot}Et_2O$ as the acid. The structure was characterized by ^1H and ^{13}C NMR and

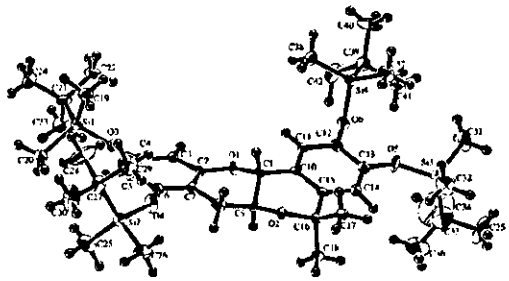

Figure 1. X-ray structure of tetra-*O*-silylated analogue (**4**) of **3**, showing ellipsoids at 50% probability.

UV−visible spectroscopy. The ^1H signals of the four protons of the phenolic OH groups showed that the catechol moiety on ring B did not react with acetone. As shown in Figure 1, the planar geometry of **3** was substantiated by single-crystal X-ray crystallography of a tetra-*O*-silylated analogue (**4**), in which the four OH groups on the A and B rings are substituted by *t*-Bu(Me)$_2$SiO groups. X-ray analysis also confirmed that the stereochemistry of 3-H on ring C was maintained throughout the reaction without any acid-catalyzed racemization.

The radical-scavenging activities of **1** and **3** as well as that of **2** were compared using galvinoxyl radical (G•) as an oxyl radical species.[14] Upon addition of **1** to a deaerated MeCN solution of G•, the absorption band at 428 nm due to G• disappeared immediately as shown in Figure 2. This indicates that hydrogen abstraction from one of the OH groups on the B ring of **1** by G• takes place to give catechin radical and hydrogenated G• (GH). The decay of the absorbance at 428 nm due to G• obeyed pseudo-first-order kinetics when the concentration of **1** was maintained at more than 10-fold excess of the G• concentration (inset of Figure 2). The dependence of the observed pseudo-first-order rate constant (k_{obs}) on the concentration of **1** is shown in Figure 3, which demonstrates a linear correlation between k_{obs} and the concentration of **1**. From the linear plot of k_{obs} vs the catechin concentration in Figure 3, we determined that the second-order rate constant (k) for hydrogen abstraction of **1** by G• was 2.34 × 10^2 M^{-1} s^{-1}. The k values for **2** and **3** were determined in the same manner to be 1.08 × 10^3 and 1.12 × 10^3 M^{-1} s^{-1}, respectively. Thus, the k value for planar catechin (**3**) is about 5-fold larger than that for catechin (**1**), approximately the same as that for quercetine (**2**).

Hydroxyl radical is the most reactive among oxygen-derived free radicals responsible for aging and free radical-mediated injury. Therefore, the effects of **1**, **2**, and **3** on hydroxyl radical-mediated

* To whom correspondence should be addressed. E-mail: fukuhara@nihs.go.jp
† National Institute of Health Sciences
‡ National Institute of Radiological Sciences, Japan Science and Technology Corporation
§ Showa Women's University
|| Shibaura Institute of Technology
⊥ Chiba University, Japan Science and Technology Corporation
Nagoya City University

10.1021/ja0178259 CCC: $22.00 © 2002 American Chemical Society

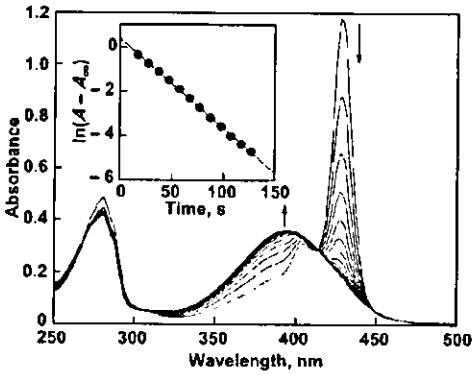

Figure 2. Spectral change in the reaction of **1** (1.5×10^{-5} M) with G• (2.4×10^{-6} M) in deaerated MeCN at 298 K (Interval: 10 s). (Inset) First-order plot based on the change in absorption at 428 nm.

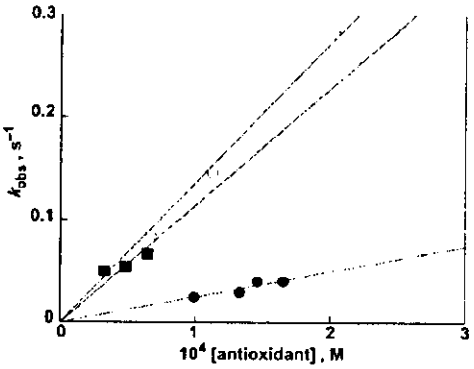

Figure 3. Plot of the pseudo-first-order rate constant (k_{obs}) vs the concentrations of **1** (●), **2** (■), and **3** (○) for hydrogen atom transfer from antioxidants to G• (2.4×10^{-6} M) in deaerated MeCN at 298 K.

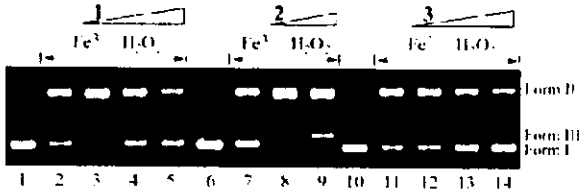

Figure 4. Effects of **1**, **2**, and **3** on DNA breakage induced by Fe^{3+}/H_2O_2. Assays were performed in 50 mM sodium cacodylate buffer, pH 7.2, containing 45 μM bp of pBR322DNA, for 1 h at 37 °C. Lanes 1, 6, and 10: DNA alone; lanes 2, 7, and 11: 10 mM H_2O_2 and 10 μM $FeCl_3$; lanes 3−5, 8, and 9, and 12−14: 10 mM H_2O_2 and 10 μM $FeCl_3$ in the presence of 0.25, 1.25, and 2.5 mM **1** (lanes 3−5), 0.25 and 1.25 mM **2**, and 0.25, 1.25 and 2.5 mM **3**.

DNA breakage were investigated. DNA-strand scission in supercoiled pBR322DNA was induced by a hydroxyl radical-generating system using hydrogen peroxide in the presence of Fe^{3+} (Fenton reaction). As shown in Figure 4, **1** at a high concentration (1.25 and 2.5 mM) suppressed DNA strand breakage, while at a low concentration (0.25 mM) it exhibited pro-oxidant properties, consistent with the enhanced DNA cleavage in comparison with cleavage without antioxidant. Quercetin (**2**) only showed pro-oxidant effects at 0.25 and 1.25 mM. In agreement with previously published results,[15] the measured pro-oxidant effects of **1** and **2** may be attributed to autoxidation of the antioxidant in the presence of transition metal, leading to the generation of primary radicals such as hydroxyl radical. In contrast to the pro-oxidant effects of **1** and **2**, the addition of **3** protected DNA from Fenton reaction-mediated damage at all of the concentrations tested, and **3** exhibited marked hydroxyl radical-scavenging ability, which exceeded that of catechin. Since **3** is very lipophilic compared to **1** (data not shown), the high radical-scavenging ability of **3** might be very useful for suppressing free-radical associated events, especially in the cell membrane.

In conclusion, we have described the first synthesis of planar catechin **3**, which was constrained by the formation of a bridge between the 3-OH group on ring C and C6′ on ring B. Preliminary experiments indicated that, despite the absence of a C2−C3 double bond, **3** showed enhanced radical-scavenging ability comparable to that of **2**. Efficient protection against DNA strand breakage induced by the Fenton reaction and the greater lipophilicity of **3** suggested that the construction of a planar catechin might be a new approach for the development of clinically useful antioxidants. The inducing planarity of **3** may pose the preferential stabilization of radicals through hyperconjugation between the π electrons on ring B and the σ electrons on C2 on ring C. In fact, a large amount of the spin density in the radical species generated via the antioxidative reaction of **3** is accumulated at the C2 position (data not shown). However, the effect of substitution to the para position from an OH ring on the B ring also should be considered as the essential factor for its enhanced reactivity. The detailed mechanism as well as the energetics of hydrogen abstraction from catechin analogues depending on the molecular structure is now under investigation.

Supporting Information Available: Experimental procedure for the preparation of **3**, kinetic measurements, the DNA-cleaving experiment, and crystallographic data for **4** (PDF). This material is available free of charge via the Internet at http://pubs.acs.org.

References

(1) (a) Katzman, R., Kawas, C. In *Alzheimer Disease*; Terry, R. D., Katzman, R., Bick, K. L., Eds.; Raven Press: New York, 1994; pp103−119. (b) Behl, C.; Davis, J. B.; Lesley, R.; Schubert, D. *Cell* **1994**, *77*, 817. (c) Butterfield, D. A. *Chem. Res. Toxicol.* **1997**, *10*, 495. (d) Huang, X.; Atwood, C. S.; Hartshorn, M. A.; Multhaup, G.; Goldstein, L. E.; Scarpa, R. C.; Cuajungco, M. P.; Gray, D. N.; Lim, J.; Moir, R. D.; Tanzi, R. E.; Bush, A. I. *Biochemistry* **1999**, *38*, 7609.

(2) (a) Olanow, C. W. *Neurology* **1990**, *40*, 37. (b) Zang, L. Y.; Misra, H. P. *J. Biol. Chem.* **1992**, *267*, 23601. (c) Pennathur, S.; Jackson Lewis, V.; Przedborski, S.; Heinecke, J. W. *J. Biol. Chem.* **1999**, *274*, 34021.

(3) (a) Mayeux, R.; Sano, M. J. *N. Engl. J. Med.* **1999**, *341*, 1670. (b) Grundman, M. *Am. J. Clin. Nutr.* **2000**, *71*, 630S.

(4) (a) Skaper, S. D.; Fabris, M.; Ferrari, V.; Carbonare, M. D.; Leon, A. *Free Radical Biol. Med.* **1997**, *22*, 669. (b) Moosmann, B.; Behl, C. *Proc. Natl. Acad. Sci. USA.* **1999**, *96*, 8867.

(5) The Parkinson Study Group *N. Engl. J. Med.* **1993**, *328*, 176.

(6) Greenspan, H. C.; Aruoma, O. I. *Immunol. Today* **1994**, *15*, 209.

(7) (a) Bors, W.; Michel, C.; Saran, M. *Methods Enzymol.* **1994**, *234*, 420. (b) Jovanovic, S. V.; Steenken, S.; Tosic, M.; Marjanovic, B.; Simic, M. G. *J. Am. Chem. Soc.* **1994**, *116*, 4846.

(8) Decharneux, T.; Dubois, F.; Beauloye, C.; Wallbanks De Cornelis, S.; Wallbanks, R. *Biochem. Pharmacol.* **1992**, *44*, 1243.

(9) Torel, J.; Cillard, J.; Cillard, P. *Phytochemistry* **1986**, *25*, 383.

(10) (a) Guo, Q.; Zhao, B.; Shen, S.; Hou, J.; Hu, J.; Bors, W.; Michel, C.; Stettmaier, K. *Arch. Biochem. Biophys.* **2000**, *374*, 347. (b) Dangles, O.; Fargeix, G.; Dufour, C. *J. Chem. Soc., Perkin Trans. 2* **2000**, 1653. (c) Valcic, S.; Burr, J. A.; Timmermann, B. N.; Liebler, D. C. *Chem. Res. Toxicol.* **2000**, *13*, 801.

(11) (a) Rice-Evans, C. A.; Miller, N. J.; Paganga, G. *Free Radical Med.* **1996**, *20*, 933. (b) van Acker, S. A. B. E.; Bast, A.; Van Der Vijgh, W. J. F. *Antioxidants Health Dis.* **1998**, 221.

(12) Van Acker, S. A. B. E.; de Groot, M. J.; van den Berg, D.-J.; Tromp, M. N. J. L.; Doone Op den Kelder, G.; van der Vijgh, W. J. F.; Bast, A. *Chem. Res. Toxicol.* **1996**, *9*, 1305.

(13) Guiso, M.; Marra, C.; Cavarischia, C. *Tetrahedron Lett.* **2001**, *42*, 6531.

(14) Goto, N.; Shimizu, K.; Komuro, E.; Tsuchiya, J.; Noguchi, N.; Niki, E. *Biochim. Biophys. Acta* **1992**, *1128*, 147.

(15) (a) Hiramoto, K.; Ojima, N.; Sako, K.; Kikugawa, K. *Biol. Pharm. Bull.* **1996**, *19*, 558−563. (b) Yamashita, N.; Tanemura, H.; Kawanishi, S. *Mutat. Res.* **1999**, *425*, 107. (c) Nakanishi, I.; Fukuhara, K.; Ohkubo, K.; Shimada, T.; Kansui, H.; Kurihara, M.; Urano, S.; Fukuzumi, S.; Miyata, N. *Chem. Lett.* **2001**, 1152.

JA0178259

Genistein and Daidzein Induce Cell Proliferation and Their Metabolites Cause Oxidative DNA Damage in Relation to Isoflavone-Induced Cancer of Estrogen-Sensitive Organs†

Mariko Murata,‡ Kaoru Midorikawa,‡ Masashi Koh,‡ Kazuo Umezawa,§ and Shosuke Kawanishi*,‡

Department of Environmental and Molecular Medicine, Mie University School of Medicine, Tsu, Mie 514-8507, Japan, and Department of Applied Chemistry, Faculty of Science and Technology, Keio University, Kohoku-Ku, Yokohama 223-8522, Japan

Received September 8, 2003; Revised Manuscript Received November 30, 2003

ABSTRACT: The soy isoflavones, genistein (5,7,4′-trihydroxyisoflavone) and daidzein (7,4′-dihydroxyisoflavone), are representative phytoestrogens that function as chemopreventive agents against cancers, cardiovascular disease, and osteoporosis. However, recent studies indicated that genistein and/or daidzein induced cancers of reproductive organs in rodents, such as the uterus and vulva. To clarify the molecular mechanisms underlying the induction of carcinogenesis by soy isoflavones, we examined the ability of genistein, daidzein, and their metabolites, 5,7,3′,4′-tetrahydroxyisoflavone (orobol), 7,3′,4′-trihydroxyisoflavone (7,3′,4′-OH-IF), and 6,7,4′-trihydroxyisoflavone (6,7,4′-OH-IF), to cause DNA damage and cell proliferation. An E-screen assay revealed that genistein and daidzein enhanced proliferation of estrogen-sensitive breast cancer MCF-7 cells, while their metabolites had little or no effect. A surface plasmon resonance sensor showed that binding of isoflavone-liganded estrogen receptors (ER) to estrogen response elements (ERE) was largely consistent with cell proliferative activity of isoflavones. Orobol and 7,3′,4′-OH-IF significantly increased 8-oxo-7,8-dihydro-2′-deoxyguanosine (8-oxodG) formation in human mammary epithelial MCF-10A cells, while genistein, daidzein, and 6,7,4′-OH-IF did not. Experiments using isolated DNA revealed a metal-dependent mechanism of oxidative DNA damage induced by orobol and 7,3′,4′-OH-IF. DNA damage was enhanced by the addition of endogenous reductant NADH, formed via the redox cycle. These findings suggest that oxidative DNA damage by isoflavone metabolites plays a role in tumor initiation and that cell proliferation by isoflavones via ER−ERE binding induces tumor promotion and/or progression, resulting in cancer of estrogen-sensitive organs.

Epidemiological and experimental studies have shown that soy products can reduce the risk of cancer (*1*−*5*) and provide other benefits including lowering cholesterol (*6, 7*) and blood pressure (*8*) and preventing cardiovascular diseases (*1, 6*) and osteoporosis (*9*). The soy isoflavones, genistein (5,7,4′-trihydroxyisoflavone) and daidzein (7,4′-dihydroxyisoflavone), are representative phytoestrogens (*10*) and act as chemopreventive agents against cancers, cardiovascular disease, and osteoporosis. Due to these health benefits, the consumption of soy food and the use of isoflavone supplements have been increasing (*11*). However, recent studies revealed that genistein and/or daidzein induced cancers of reproductive organs in rodents, such as the uterus (*12*) and vulva (*13*). In addition, genistein was reported to have tumor-enhancing effects on breast (*14*) and colon cancer (*15*). Dietary soy increased the rate of epithelial proliferation in histologically normal human breasts in premenopausal women (*16*). A stimulatory influence of soy on breast secretion and hyperplastic epithelial cells was also observed in pre- and postmenopausal women (*17*). These reports led us to consider that soy isoflavones may have a carcinogenic effect on female reproductive organs.

Epidemiological studies and animal experiments suggest that estrogens have carcinogenic actions in humans (*18, 19*). Recent meta analyses have revealed that users of postmenopausal estrogen as hormone replacement therapy have an increased risk of breast and endometrial cancer (*20*). According to the hypothesis of estrogen-induced carcinogenesis (*21, 22*), catechol estrogens, which are metabolites of estrogen, play a role in tumor initiation through oxidative DNA damage, whereas estrogen itself induces tumor promotion and/or progression by enhancing cell proliferation. Therefore, there arises the possibility that genistein, daidzein, and their metabolites may participate in tumor initiation and promotion by causing DNA damage and cell proliferation, thereby leading to carcinogenesis. Like endogenous estrogens, genistein and daidzein may have the capacity to produce not only beneficial actions but also adverse effects including carcinogenesis.

To investigate whether soy isoflavones affect tumor initiation and promotion, we investigated DNA damage and cell proliferative activity induced by genistein, daidzein, and their metabolites. The chemical structures of the isoflavones and their metabolites tested are shown in Figure 1. These metabolites have been detected as products of oxidative

† This work was supported by Grants-in-Aid for Scientific Research on Priority Areas (A) from the Ministry of Education, Science, Sports, and Culture of Japan (14042227).

* To whom correspondence and requests for reprints should be addressed. Phone/Fax: +81-59-231-5011. E-mail: kawanisi@doc.medic.mie-u.ac.jp.

‡ Mie University School of Medicine.

§ Keio University.

10.1021/bi035613d CCC: $27.50
Published on Web 02/10/2004

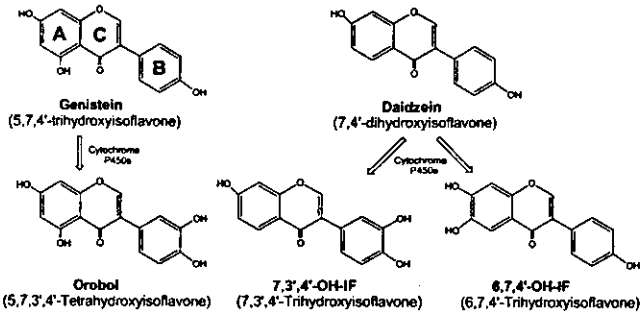

FIGURE 1: Chemical structures of isoflavones (genistein, daidzein) and their metabolites used in this study.

metabolism of genistein and daidzein, in vitro and in vivo (*23*, *24*). We examined the effects of these substances on cell proliferation of estrogen-dependent MCF-7 cells, using an E-screen assay. Furthermore, to study interactions between isoflavone-liganded estrogen receptors and estrogen response elements, we measured binding affinity using a surface plasmon resonance (SPR) sensor. Formation of 8-oxo-7,8-dihydro-2′-deoxyguanosine (8-oxodG),[1] an indicator of oxidative damage, in human mammary epithelial cells treated with genistein, daidzein, and their metabolites, was measured using an electrochemical detector coupled to HPLC (HPLC-ECD). To elucidate the mechanism of DNA damage, we measured 8-oxodG formation in calf thymus DNA and examined DNA damage using ^{32}P-5′-end-labeled DNA fragments obtained from the human *p53* and *p16* tumor suppressor genes and the c-Ha-*ras*-1 protooncogene.

MATERIALS AND METHODS

Materials. Restriction enzymes (*Sma*I, *Eco*RI, *Bss*HII, *Apa*I, and *Sty*I) and proteinase K were purchased from Roche Molecular Biochemicals (Mannheim, Germany). Restriction enzymes (*Hin*dIII, *Ava*I, and *Xba*I) and T_4 polynucleotide kinase were purchased from New England Biolabs (Beverly, MA). [γ-^{32}P]ATP (222 TBq/mmol) was obtained from New England Nuclear (Boston, MA). Genistein was purchased from Wako Chemical Co. (Osaka, Japan). We isolated orobol (5,7,3′,4′-tetrahydroxyisoflavone), one of the metabolites of genistein, from *Streptomyces* according to a method described previously (*25*). 7,3′,4′-Trihydroxyisoflavone (7,3′,4′-OH-IF) and 6,7,4′-trihydroxyisoflavone (6,7,4′-OH-IF), which are metabolites of daidzein, were obtained from Extrasynthèse (Genay, France). β-Nicotinamide adenine dinucleotide disodium salt (reduced form) (NADH) was purchased from Kohjin Co. (Tokyo, Japan). Diethylenetriamine-*N*,*N*,*N*′,*N*″,*N*″-pentaacetic acid (DTPA) and bathocuproinedisulfonic acid were obtained from Dojin Chemicals Co. (Kumamoto, Japan). Fetal bovine serum (FBS), horse serum (HS), epidermal growth factor (EGF), Dulbecco's modified Eagle medium (DMEM), and Ham's F12 medium were purchased from Gibco (Grand Island, NY). Daidzein, superoxide dismutase (SOD, 3000 units/mg from bovine erythrocytes), catalase (45000 units/mg from bovine liver), L-buthionine (*S*,*R*)-sulfoximine (BSO), bacterial alkaline phosphatase, RNase A, phenol red free DMEM, insulin, hydrocortisone, and charcoal (activated) were purchased from Sigma Chemical Co. (St. Louis, MO). Formamidopyrimidine−DNA glycosylase (Fpg, 20000 units/mg from *Escherichia coli*) was from Trevigen Inc. (Gaithersburg, MD). Lysis buffer for DNA extraction (model 340A) was purchased from Applied Biosystems (Foster City, CA). 17β-Estradiol (E_2) was obtained from Calbiochem-Novabiochem Corp. (La Jolla, CA). Dimethyl sulfoxide (DMSO) and kanamycin sulfate were from Wako Chemical Co. (Osaka, Japan). L-Glutamine was from ICN Biomedicals Inc. (Aurora, OH). Dextran T70 was from Pharmacia Biotech (Uppsala, Sweden). The BIAcore sensor chips SA (modified with streptavidin) were obtained from Biacore Inc. (Uppsala, Sweden). Tween 20 was from Nacalai Tesque (Kyoto, Japan). Human recombinant estrogen receptor α (ERα) and estrogen receptor β (ERβ) were obtained from Panvera (Madison, WI).

Cell Culture. Human estrogen-sensitive breast cancer MCF-7 cells (ATCC No. HTB 22) and nontumorigenic mammary epithelial MCF-10A cells (ATCC No. CRL 10317) were obtained from American Type Culture Collection (Dainippon Pharmaceutical Co., Osaka, Japan). For routine maintenance, cells were grown in seeding medium (MCF-7 cells, DMEM supplemented with 100 ng/mL kanamycin and 5% FBS; MCF-10A cells, DMEM/F12 supplemented with 20 ng/mL EGF, 0.01 mg/mL insulin, 500 ng/mL hydrocortisone, 100 ng/mL kanamycin, and 5% HS) at 37 °C in a humidified atmosphere of 5% CO_2. Sex steroids in serum were removed by charcoal−dextran treatment for experimental medium by the method reported previously (*21*). Experimental medium was phenol red free medium supplemented with 5% charcoal−dextran−serum, 100 ng/mL kanamycin, and 4 mM L-glutamine.

Bioassay for Measuring Estrogenic Activity (E-Screen Assay). The E-screen assay was performed by a modified method of Soto et al. (*26*). Briefly, MCF-7 cells were trypsinized and plated into 12-well plates at an initial concentration of 3×10^4 cells per well with seeding medium. After the cells were allowed to attach for 24 h, the seeding medium was replaced with experimental medium. A range of concentrations (10^{-10}−10^{-5} M) of the test compounds was added. 17β-Estradiol (E_2) and isoflavones were dissolved in DMSO before being tested. The final solvent concentration in culture medium did not exceed 0.1%, as this concentration did not affect cell yields (*26*). The control condition also contained 0.1% DMSO. Cells were incubated for 6 days after treatment with the test compounds and were then trypsinized and harvested. Harvested cells were counted using a Coulter counter (Beckman Coulter, Tokyo, Japan).

Preparation of the Sensor Chip and Immobilization of ERE. The single-stranded biotinylated oligonucleotide (35mer, HPLC grade), containing the sequence of human *pS2* ERE (*27*), and the complementary unbiotinylated oligonucleotide (35mer, HPLC grade) were obtained from TaKaRa Biotechnology Co., Ltd. (Shiga, Japan). The sequence is 5′-XGTCCAAAGTCAGGTCACGGTGGCCTGATCAAAGTT-3′ (X indicates biotin-labeled). Oligonucleotides were biotinylated for immobilization to the streptavidin-treated sensor chip. The BIAcore-biosensor system (Biacore X,

[1] Abbreviations: Orobol, 5,7,3′,4′-tetrahydroxyisoflavone; 7,3′,4′-OH-IF, 7,3′,4′-trihydroxyisoflavone; 6,7,4′-OH-IF, 6,7,4′-trihydroxyisoflavone; E_2, 17β-estradiol; ER, estrogen receptor; ERE, estrogen response element; 8-oxodG, 8-oxo-7,8-dihydro-2′-deoxyguanosine; HPLC-ECD, electrochemical detector coupled to HPLC; DTPA, diethylenetriamine-*N*,*N*,*N*′,*N*″,*N*″-pentaacetic acid; SOD, superoxide dismutase; DMEM, Dulbecco's modified Eagle medium; F12, Ham's F12 medium; FBS, fetal bovine serum; HS, horse serum; ·OH, hydroxyl radical; H_2O_2, hydrogen peroxide; BSO, buthionine sulfoximine.

Pharmacia Biosensor, Uppsala, Sweden) permits the monitoring of macromolecular interactions in real time using a surface plasmon resonance (SPR) sensor (*28*). The running buffer used for immobilization and the binding assay consisted of 25 mM Tricine, 160 mM KCl, 5 mM $MgCl_2$, and 0.05% Tween 20 (pH 7.8). Before immobilization of biotinylated ERE, the surface of the SA (streptavidin-treated) sensor chip was washed with five 5 μL injections of 100 mM NaOH and 50 mM HCl each with a constant flow of running buffer of 20 μL/min. For denaturation, oligonucleotides were heated at 105 °C for 5 min and then chilled on ice before immobilization. 5′-End-biotinylated single-stranded oligonucleotides (Human *pS2* ERE) diluted with running buffer were immobilized to a flow cell (Fc2) of an SA sensor chip at about 200 RU by serial 5 μL injection with a constant flow of running buffer of 5 μL/min. Then, the sensor chip surface was blocked by biotin, followed by five washes with NaOH and HCl. The complementary oligonucleotide was annealed to the immobilized ERE by a 10 μL injection.

Analysis of ER−ERE Binding. Incubating at 37 °C for 5 min liganded human ERα and ERβ (2×10^{-7} M) with 10^{-7} M E_2 or 10^{-5} M isoflavones and their metabolites. Then, the liganded ER was introduced by a 40 μL injection over the surfaces coated with double-stranded ERE via a sample loop. Each binding cycle was performed with a constant flow of buffer of 20 μL/min at 25 °C. ER protein was injected during the "binding" phase, and running buffer was injected across the flow cells during the "dissociating" phase for 120 s. As significant amounts of ER were still bound to the ERE at the end of the injection, the complementary oligonucleotide was removed with a 5 μL injection of 100 mM NaOH and 50 mM HCl, each with a constant flow of running buffer of 20 μL/min for regeneration. Data were collected as the subtracted curve (Fc1 − Fc2) at 1 Hz. The binding activity of liganded ER to ERE was expressed as percent activity, that is, binding response with 100 nM E_2 as 100% and that without chemical (DMSO, 0.1%) as 0%. All samples contained 0.1% DMSO.

Measurement of 8-OxodG in DNA from Cultured Human Mammary Epithelial Cells Treated with Genistein, Daidzein, and Their Metabolites. Human mammary epithelial cells (MCF-10A cells and MCF-7 cells) were trypsinized, and 5×10^5 cells were plated into a 10 cm diameter dish with seeding medium. Cells were allowed to attach and grow until 70−90% confluency for 3−4 days. Then, cells were treated with isoflavones at 37 °C for 1 h and trypsinized and washed three times with cold PBS. Under anaerobic conditions, DNA was extracted using lysis buffer, RNase A, and proteinase K. After ethanol precipitation, DNA was digested to component nucleosides with nuclease P_1 and bacterial alkaline phosphatase and then analyzed by HPLC-ECD as previously described (*29*). In certain experiments, breast cancer MCF-7 cells were pretreated with an inhibitor of GSH biosynthesis (BSO, 100 μM, 18 h) to decrease GSH levels to that of normal mammary cells.

Measurement of GSH Content in MCF-10A and MCF-7 Cells. Cells were washed twice with PBS, followed by addition of 100 μL/10^6 cells of 5% (w/v) trichloroacetic acid to precipitate proteins. Then, cells were homogenized for 5 s with a microhomogenizer with a Teflon-coated pestle and centrifuged at 18500*g* for 10 min at 4 °C. The supernatant was diluted with 0.1 N HCl, and levels of GSH were quantitated with an HPLC-ECD using a gold electrode (Eicom, Kyoto, Japan), as described previously (*30*).

Analysis of 8-OxodG Formation in Calf Thymus DNA by Genistein, Daidzein, and Their Metabolites in the Presence of NADH and Cu(II). DNA fragments (100 μM per base) from calf thymus were incubated with isoflavones, Cu(II), and NADH at 37 °C for the indicated times. DNA fragments were denatured by heating at 90 °C for 5 min, followed by chilling on ice before incubation. After ethanol precipitation, DNA was digested to the nucleosides with nuclease P_1 and calf intestine phosphatase and then analyzed by HPLC-ECD, as described previously (*29*).

Preparation of ^{32}P-5′-End-Labeled DNA Fragments. Exon-containing DNA fragments obtained from the human *p53* tumor suppressor gene (*31*) were prepared as described previously (*32*). A 5′-end-labeled 650 bp fragment (*Hin*dIII* 13972−*Eco*RI* 14621) was obtained by dephosphorylation with calf intestine phosphatase and rephosphorylation with [γ-^{32}P]ATP and T_4 polynucleotide kinase (*, ^{32}P-label). The 650 bp fragment was further digested with *Apa*I to obtain a singly labeled 443 bp fragment (*Apa*I 14179−*Eco* RI* 14621) and a 211 bp fragment (*Hin*dIII* 13972−*Apa*I 14182). The fragment was prepared from plasmid pbcNI, which carries a 6.6 kb *Bam*HI chromosomal DNA segment containing the c-Ha-*ras*-1 protooncogene (*33*). A singly labeled 98 bp fragment (*Ava*I* 2247−*Pst*I 2344) was obtained according to the method described previously (*34*). Nucleotide numbering starts with the *Bam*HI site (*33*).

Detection of DNA Damage by Genistein, Daidzein, and Their Metabolites in the Presence of NADH and Cu(II). A standard reaction mixture (in a 1.5 mL Eppendorf microtube) contained the isoflavones, Cu(II), NADH, ^{32}P-5′-end-labeled DNA fragments, and calf thymus DNA (5−10 μM per base) in 200 μL of 10 mM sodium phosphate buffer (pH 7.8) containing 2.5 μM DTPA. After incubation at 37 °C for the indicated times, the DNA fragments were heated at 90 °C in 1 M piperidine for 20 min, where indicated, and treated as described previously (*35*). In certain experiments, the DNA was treated with 6 units of Fpg protein in 10 μL of reaction buffer [10 mM HEPES−KOH (pH 7.4), 100 mM KCl, 10 mM EDTA, and 0.1 mg/mL BSA] at 37 °C for 2 h. The preferred cleavage sites were determined by direct comparison of the labeled, cleaved oligonucleotides with a standard 5′-end-labeled Maxam−Gilbert sequencing reaction (*36*) (LKB 2010 Macrophor, LKB Pharmacia Biotechnology Inc.). The relative amounts of oligonucleotides from the treated DNA fragments were measured with a laser densitometer (LKB 2222 UltroScan XL, LKB Pharmacia Biotechnology Inc.).

RESULTS

Cell Proliferative Activity of Genistein and Daidzein in MCF-7 Cells. The effects of isoflavones and their metabolites on cell proliferation were measured by an E-screen assay. Genistein induced maximal proliferative activity at 10^{-6} M ($P < 0.01$), with significant differences relative to solvent control (0.1% DMSO) starting at 10^{-7} M ($P < 0.05$) (Figure 2A). The intensity of maximal estrogenic activity of genistein was about 90% of estradiol. Orobol showed a significant proliferative activity at 10^{-5} M ($P < 0.05$). Daidzein showed

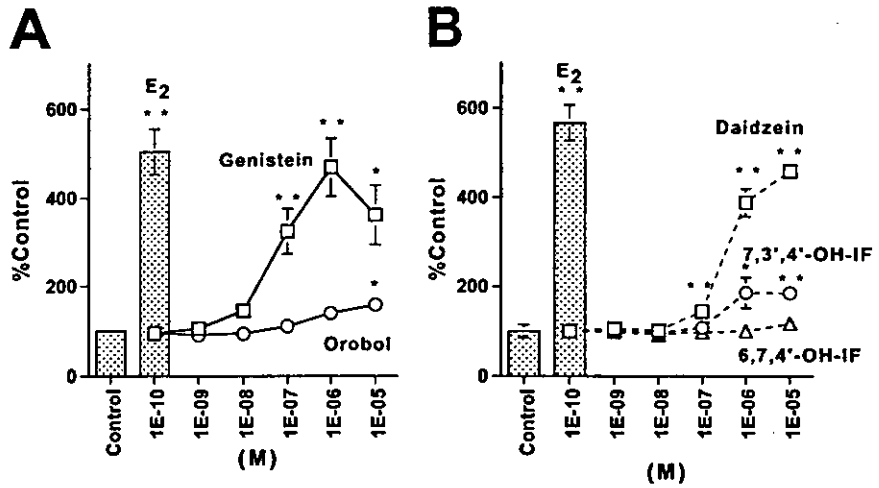

FIGURE 2: Relative estrogenic activities of isoflavones and their metabolites. MCF-7 cells were incubated with genistein, orobol (A), daidzein, 7,3′,4′-OH-IF, or 6,7,4′-OH-IF (B) at 37 °C for 6 days. Cells were trypsinized, harvested, and then counted. Results are expressed as means and SE of values obtained from six to nine independent experiments. Key: *, $P < 0.05$, and **, $P < 0.01$; significant difference compared with the control by Student's *t*-test.

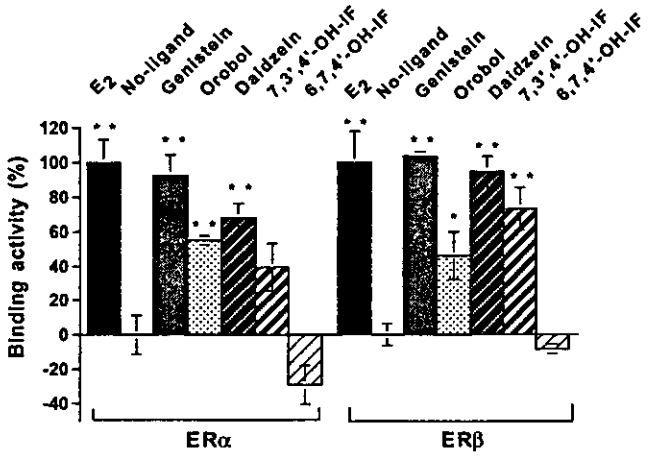

FIGURE 3: ER−ERE binding activities in the presence of isoflavones and their metabolites. Human ERα and ERβ (20 nM) were liganded with 100 nM E_2 or 10 μM phytoestrogens by incubation at 37 °C for 5 min. Then, the liganded ER was introduced by a 40 μL injection over the sensor chip surface immobilized with double-stranded human *pS2* ERE. The binding activity of liganded ER to ERE was expressed as percent activity, that is, binding response with 100 nM E_2 as 100% and no ligand (DMSO, 0.1%) as 0%. Results are expressed as means and SE of percent activity obtained from three independent experiments. Key: *, $P < 0.05$, and **, $P < 0.01$; significant difference compared with the no ligand condition by Student's *t*-test.

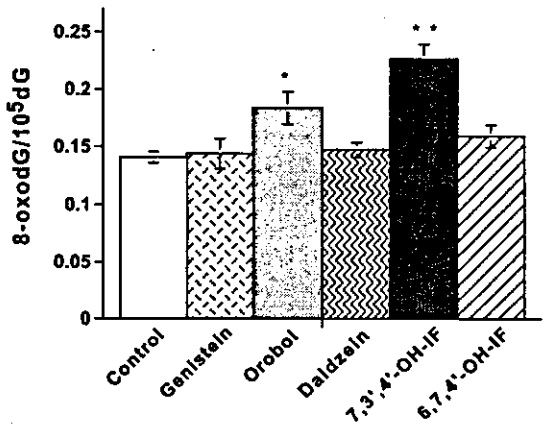

FIGURE 4: Intracellular 8-oxodG formation by isoflavone metabolites in MCF-10A cells. MCF-10A cells were treated with 10 μM isoflavones or their metabolites in the experimental medium at 37 °C for 1 h. Results are expressed as means and SE of values obtained from three independent experiments. Key: *, $P < 0.05$, and **, $P < 0.01$; significant difference compared with the control by Student's *t*-test.

maximal proliferative activity at 10^{-5} M ($P < 0.01$), with significant differences relative to controls starting at 10^{-7} M ($P < 0.05$) (Figure 2B). Daidzein exhibited an estrogenicity about 80% that of estradiol. 7,3′,4′-OH-IF showed significant proliferative activity at 10^{-6} and 10^{-5} M. 6,7,4′-OH-IF had no significant proliferative effect.

Binding of Isoflavone-Liganded ERα and ERβ to ERE. The binding activity of liganded ER to ERE was measured by using an SPR sensor (Figure 3). Genistein- and daidzein-liganded ER had significantly elevated binding activity, as did E_2. The binding activity of liganded ERβ was slightly higher than that of ERα. Binding activity was also detected for the metabolites, orobol and 7,3′,4′-OH-IF, but it was lower than in the parent isoflavones. On the other hand, 6,7,4′-OH-IF attenuated binding to ERE, although there was no significant difference relative to nonliganded ER. Similar results were obtained with ERα and ERβ.

Induction of 8-OxodG Formation in Human Cultured Mammary Cells Treated with Isoflavone Metabolites. Orobol and 7,3′,4′-OH-IF significantly increased 8-oxodG formation in normal mammary epithelial MCF-10A cells, but no significant increase was observed in cells treated with genistein, daidzein, or 6,7,4′-OH-IF (Figure 4). In contrast, there was no significant increase in 8-oxodG formation in MCF-7 breast cancer cells treated with isoflavones and their metabolites compared to controls (data not shown). The GSH level in MCF-7 cells was 2-fold higher than in MCF-10A cells (data not shown). The GSH level decreased to 50% in MCF-7 cells following pretreatment with BSO, and thereafter, significant increases were observed in MCF-7 cells treated with orobol and 7,3′,4′-OH-IF (data not shown).

Formation of 8-OxodG in Calf Thymus DNA by Isoflavone Metabolites in the Presence of Cu(II) and NADH. Cu(II)-mediated 8-oxodG formation in calf thymus DNA treated with isoflavones, in the presence and absence of NADH, was examined using HPLC-ECD (Figure 5). In the case of

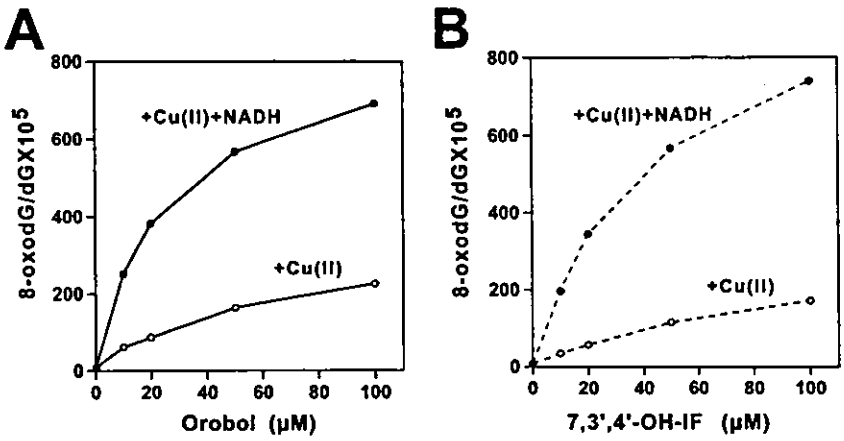

FIGURE 5: Formation of 8-oxodG in calf thymus DNA treated with isoflavone metabolites in the presence of Cu(II) and NADH. The reaction mixture contained 100 μM/base calf thymus DNA, the indicated concentrations of orobol (A) or 7,3′,4′-OH-IF (B), 20 μM $CuCl_2$, and no or 200 μM NADH in 4 mM phosphate buffer (pH 7.8) containing 1 μM DTPA. After incubation at 37 °C for 1 h, 0.1 mM DTPA was added to stop the reaction, and DNA was precipitated in ethanol and enzymatically digested into nucleosides. Then, the levels of 8-oxodG were quantitated by HPLC-ECD.

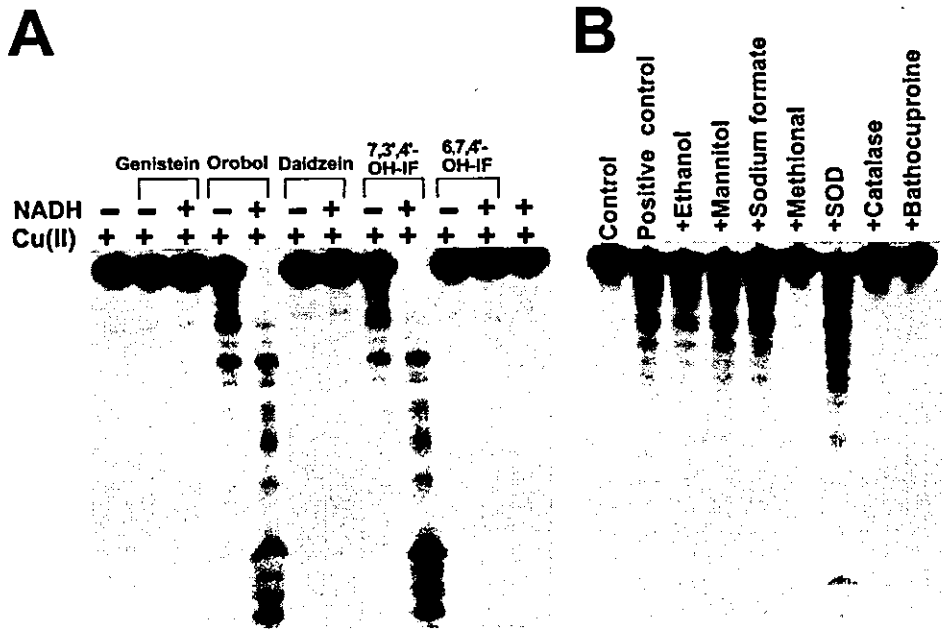

FIGURE 6: Autoradiogram of ^{32}P-labeled DNA fragments incubated with isoflavones in the presence of Cu(II) and NADH and the effects of scavengers. (A) The reaction mixture contained the ^{32}P-5′-end-labeled 261 bp DNA fragment, 20 μM/base thymus DNA, 100 μM isoflavones, 20 μM $CuCl_2$, and 200 μM NADH in 10 mM phosphate buffer (pH 7.8) containing 2.5 μM DTPA. (B) The reaction mixtures contained the ^{32}P-5′-end-labeled 211 bp DNA fragment, 20 μM/base sonicated calf thymus DNA, 100 μM 7,3′,4′-OH-IF, and 20 μM $CuCl_2$ in 10 mM phosphate buffer (pH 7.8) containing 2.5 μM DTPA. Scavenger or bathocuproine was added as follows: 5% ethanol, 0.1 M mannitol, 0.1 M sodium formate, 0.1 M methional, 150 units/mL SOD, 150 units/mL catalase, and 50 μM bathocuproine. The mixtures were incubated for 1 h at 37 °C. The DNA fragments were treated with 1 M piperidine for 20 min at 90 °C and then electrophoresed on an 8% polyacrylamide/8 M urea gel. The autoradiogram was obtained by exposing an X-ray film to the gel.

genistein, daidzein, and 6,7,4′-OH-IF, no increase in 8-oxodG formation was observed, even in the presence of NADH and Cu(II) (data not shown). Conversely, the level of 8-oxodG increased in parallel with concentrations of orobol (Figure 5A) and 7,3′,4′-OH-IF (Figure 5B) in the presence of Cu(II). When a physiological concentration of NADH (200 μM) (*37*) was added, 2−3-fold increases in 8-oxodG formation were observed. The metabolites with 3′- and 4′-positions of the hydroxy group in the B ring of the isoflavone structure caused oxidative DNA damage.

Damage to ^{32}P-Labeled DNA Fragments by Isoflavone Metabolites in the Presence of Cu(II) and NADH. Figure 6A shows an autoradiogram of DNA fragments treated with isoflavones and their metabolites in the presence and absence of Cu(II) and NADH. Oligonucleotides were detected on the autoradiogram following DNA cleavage. Genistein, daidzein, and 6,7,4′-OH-IF caused no DNA damage, even in the presence of Cu(II) and NADH. Orobol and 7,3′,4′-OH-IF caused DNA damage in the presence of Cu(II). The intensity of DNA damage increased with successive concentrations of the metabolites (data not shown). When NADH was added, Cu(II)-mediated DNA damage was enhanced. When Fe(III)EDTA was used in place of Cu(II), slight DNA damage was observed (data not shown), indicating the crucial role of metal ions. The catechol-type metabolites caused Cu(II)-mediated oxidative DNA damage, whereas genistein and daidzein did not, even in the presence of Cu(II) and NADH, as seen in the measurement of 8-oxodG content.

Effects of Scavengers and Bathocuproine on DNA Damage by Isoflavone Metabolites. Figure 6B shows the effects of scavengers and bathocuproine, a Cu(I)-specific chelator, on DNA damage induced by 7,3′,4′-OH-IF in the presence of Cu(II). Inhibition of DNA damage by catalase and bathocuproine suggests the involvement of hydrogen peroxide (H_2O_2) and Cu(I). Methional reduced the amount of DNA damage, although other typical hydroxyl radical (•OH) scavengers, ethanol, mannitol, and sodium formate did not decrease damage. Furthermore, SOD had no effect on DNA damage. In the case of the genistein metabolite orobol, similar effects of scavengers were observed (data not shown).

Site Specificity of DNA Cleavage by Isoflavone Metabolites. Isoflavone metabolites/Cu(II) caused little strand breakage, as detected without treatment (Figure 7A, lane 2, and Figure 7E). In addition, an increase in the number of oligonucleotides following piperidine treatment suggested that metabolites caused base modification/ liberation (Figure 7A, lane 4). Fpg treatment increased oligonucleotides, indicating the formation of 8-oxoG and other oxidized bases (Figure 7A, lane 6). To examine site specificity, an autoradiogram was obtained and scanned with a laser densitometer to measure the relative intensity of DNA cleavage in the human c-Ha-*ras*-1 protooncogene and *p53* tumor suppressor gene. Orobol/Cu(II)/NADH induced piperidine-labile sites preferentially at thymine residues and Fpg-sensitive sites at guanine residues in the 5′-TG-3′ sequence of the c-Ha-*ras*-1 gene (Figure 7B,C). Fpg treatment induced significant cleavage of the guanine residue of the ACG sequence complementary to codon 273, a well-known hot spot (*38*, *39*) in the *p53* gene (Figure 7G). Piperidine treatment cleaved cytosine and guanine residues at the ACG (Figure 7F) to some extent. Similar results were obtained with 7,3′,4′-OH-IF (data not shown).

DISCUSSION

The present study showed that genistein and daidzein exerted cell proliferative activity on estrogen-sensitive MCF-7 cells, as reported previously (*40*, *41*), while their metabolites had little or no activity. In accordance with the data on cell proliferation, the SPR sensor showed that genistein and daidzein induced higher affinity binding of ER to ERE, while the metabolites had little or no binding activity. Although Cheskis et al. (*42*) showed that SPR was available for a binding assay of estrogen-liganded ER−ERE, we further demonstrated that an SPR sensor could estimate the potency of environmental estrogens. Genistein (5,7,4′-trihydroxyisoflavone) and daidzein (7,4′-trihydroxyisoflavone) have similar chemical structures to endogenous estrogens. Their structural similarity to estrogens permits binding with ER (*27*). The 4′-hydroxy position on the B ring and its spatial orientation relative to the 7-hydroxy group on ring A are primarily responsible for the estrogenic activity of flavonoids (*43*). Excessive hydroxyl groups in ring B at the 3′-position, as in orobol (5,7,3′,4′-tetrahydroxyisoflavone) and 7,3′,4′-OH-IF, is thought to attenuate the binding of ER and ERE. A hydroxyl group in ring A at the 6-position, as in 6,7,4′-OH-IF, shows a similar effect. Our results further supported that isoflavones such as genistein and daidzein may induce cell proliferation through ER−ERE binding. Kuiper et al. (*44*) showed that the relative binding affinity of genistein to ERβ was significantly higher (about 20-fold) than ERα, whereas Nikov et al. (*45*) demonstrated slightly higher affinity between ERE and isoflavone-saturated ERβ than with ER α, using fluorescence polarization. The latter data are consistent with our results using an SPR biosensor that showed slightly higher affinity of isoflavone-liganded ERβ than ERα to ERE. The results from the E-screen assay and binding assay were almost coincident with little discrepancy. Orobol and 7,3′,4′-OH-IF bound relatively efficiently to both estrogen receptors but only poorly stimulated cell proliferation in MCF-7 cells. This may be explained by the difference between physicochemical responses and biological systems with a threshold range. In addition, Wong et al. (*46*) have reported that nuclear receptor ligands can be functionally selective and may differentially affect the interaction of receptors with coactivators and/or corepressors to initiate transcription. Endogenous estrogens cause cancer by stimulating cell proliferation through ER−ERE binding (*47*, *48*). Similarly, these estrogen-like substances can be mitogenic in estrogen-sensitive tissues such as uterus and breast, which may contribute to tumor promotion.

Van Duursen et al. (*49*) demonstrated that constitutive CYP1A1 activity was very low in both MCF-7 and MCF-10A cells. In addition, Price et al. (*50*) showed that the optimal time for induction of metabolism by a CYP1A inducer was 72 h in rat hepatocytes. Therefore, metabolism in cultured cells was negligible under our experimental design (1 h incubation). This may explain why genistein and daidzein themselves did not induce DNA damage. On the other hand, the addition of the isoflavone metabolites, orobol and 7,3′,4′-OH-IF, caused oxidative DNA damage. Possible mechanisms of oxidative DNA damage mediated by metabolites of genistein and daidzein can be envisioned on the basis of our results. Dihydroxy forms of the isoflavone metabolites, orobol and 7,3′,4′-OH-IF, can be autoxidized to semiquinone radicals and further to quinone forms. Generation of $O_2^{\bullet -}$ would then occur, coupled with the autoxidation of metabolites. Thereafter, $O_2^{\bullet -}$ is dismutated to generate H_2O_2. In the presence of metal ions, H_2O_2 causes oxidative DNA damage. Inhibitory effects of catalase and bathocuproine on DNA damage by the metabolites suggest that H_2O_2 and Cu(I) participate in DNA damage. Although typical •OH scavengers showed no inhibitory effects on DNA damage, methional attenuated DNA damage, suggesting the involvement of reactive species such as Cu(I)−hydroperoxo complexes that are less reactive than •OH (*51*). The addition of NADH efficiently enhanced oxidative DNA damage by isoflavone metabolites. This can be explained by our results and those of our previous studies (*21*, *52*, *53*). NADH reduces quinone forms and semiquinone radicals to dihydroxy forms, resulting in enhanced generation of reactive oxygen species and DNA damage through the redox cycle. It is interesting that Fpg and piperidine treatment revealed that orobol and 7,3′,4′-OH-IF can affect the cytosine and guanine of the ACG sequence complementary to codon 273, a hot spot in the *p53* gene.

Oxidative DNA damage plays an important role in carcinogenesis (*54*). Orobol and 7,3′,4′-OH-IF significantly induced 8-oxodG formation in MCF-10A cells, and in MCF-7 cells with GSH levels decreased to 50% with BSO treatment. Normal human breast tissue has a lower GSH content than breast tumor (*55*). Therefore, the depletion of GSH by BSO in MCF-7 cells may provide an insight into

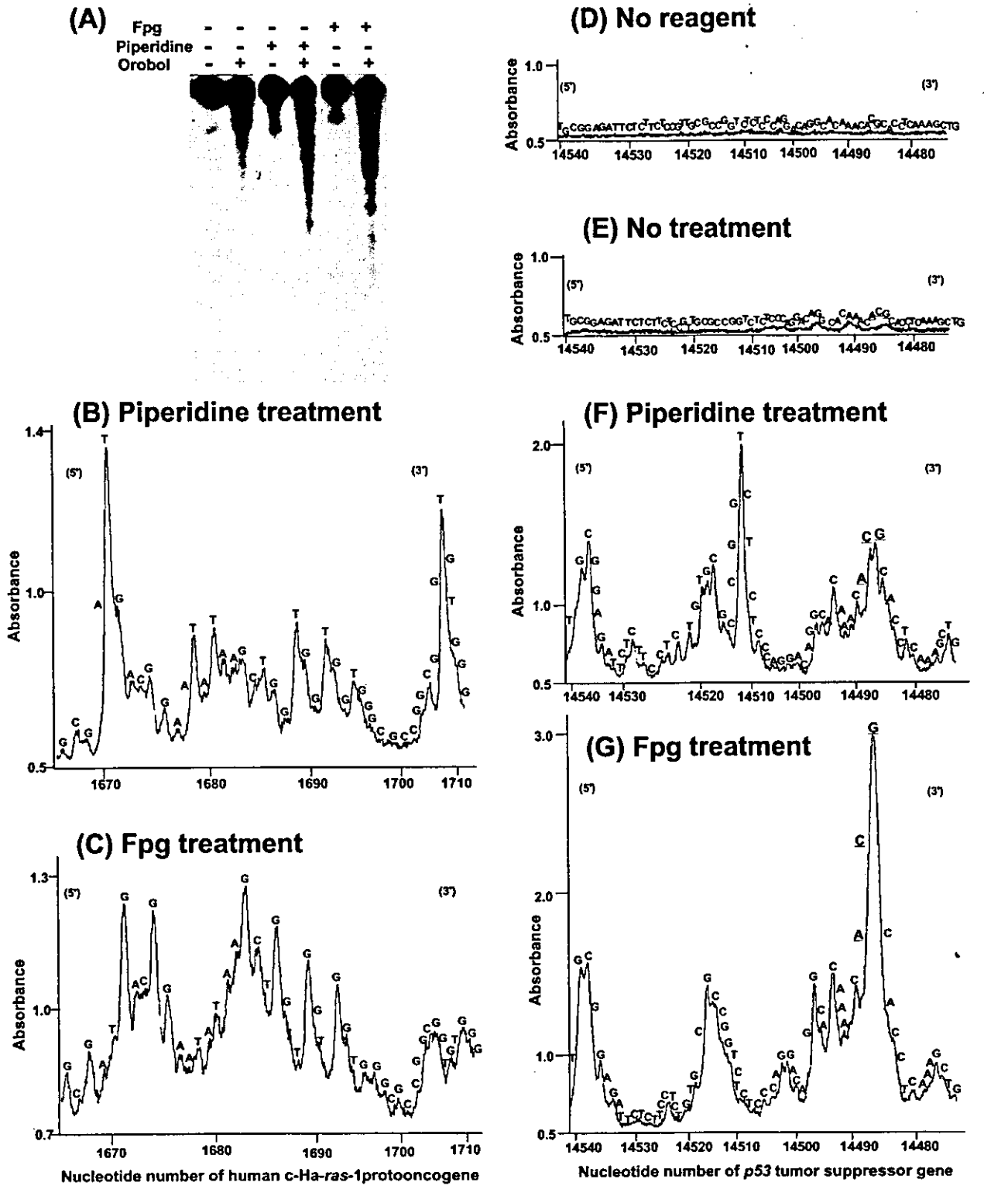

FIGURE 7: Site specificity of DNA cleavage induced by isoflavone metabolites in the presence of Cu(II) and NADH. The reaction mixture contained the ^{32}P-5′-end-labeled 261 bp (*Ava*I* 1645−*Xba*I 1905) (B, C) or 443 bp (*Apa*I 14179−*Eco*RI* 14621)(A, D−G) DNA fragment, 20 μM/base calf thymus DNA, 5 μM orobol, 20 μM $CuCl_2$, and 200 μM NADH in 10 mM phosphate buffer (pH 7.8) containing 2.5 μM DTPA. After incubation for 1 h at 37 °C, the DNA fragments were treated with piperidine (A, B, D, F) or Fpg protein (A, C, G) and electrophoresed by the method described in Materials and Methods. The relative amounts of DNA fragments were measured by scanning the autoradiogram with a laser densitometer (B−G). The horizontal axis shows the nucleotide number of the c-Ha-*ras*-1 protooncogene (B, C) and the human *p53* tumor suppressor gene (D−G), and underscoring shows the complementary sequence to codon 273 (nucleotide numbers 14486−14488).

normal breast tissue condition. Several studies showed increased formation of 8-oxodG in breast cancer tissue from patients relative to noncancerous breast tissue from controls (*56*, *57*), suggesting that accumulation of 8-oxodG in DNA is a major contributor to breast carcinogenesis. The present results and literature thus indicate that oxidative DNA damage by isoflavone metabolites plays a role in tumor initiation and cell proliferation by isoflavones via ER−ERE

binding induces tumor promotion and/or progression, resulting in cancer of estrogen-sensitive organs. Our study raises the possibility that genistein and daidzein are carcinogenic in estrogen-sensitive organs, even though isoflavones are generally regarded as chemopreventive agents.

REFERENCES

1. Knight, D. C., and Eden, J. A. (1996) A review of the clinical effects of phytoestrogens, *Obstet. Gynecol. 87*, 897−904.
2. Nagata, C., Takatsuka, N., Kawakami, N., and Shimizu, H. (2002) A prospective cohort study of soy product intake and stomach cancer death, *Br. J. Cancer 87*, 31−36.
3. Lamartiniere, C. A., Cotroneo, M. S., Fritz, W. A., Wang, J., Mentor-Marcel, R., and Elgavish, A. (2002) Genistein chemoprevention: timing and mechanisms of action in murine mammary and prostate, *J. Nutr. 132*, 552S−558S.
4. Thiagarajan, D. G., Bennink, M. R., Bourquin, L. D., and Kavas, F. A. (1998) Prevention of precancerous colonic lesions in rats by soy flakes, soy flour, genistein, and calcium, *Am. J. Clin. Nutr. 68* (Suppl. 6), 1394S−1399S.
5. Upadhyaya, P., and El-Bayoumy, K. (1998) Effect of dietary soy protein isolate, genistein, and 1,4-phenylenebis(methylene)selenocyanate on DNA binding of 7,12-dimethylbenz[*a*]anthracene in mammary glands of CD rats, *Oncol. Rep. 5*, 1541−1545.
6. Sirtori, C. R., Lovati, M. R., Manzoni, C., Monetti, M., Pazzucconi, F., and Gatti, E. (1995) Soy and cholesterol reduction: clinical experience, *J. Nutr. 125* (Suppl. 3), 598S−605S.
7. Carroll, K. K., and Kurowska, E. M. (1995) Soy consumption and cholesterol reduction: review of animal and human studies, *J. Nutr. 125* (Suppl. 3), 594S−597S.
8. Rivas, M., Garay, R. P., Escanero, J. F., Cia, P., Jr., Cia, P., and Alda, J. O. (2002) Soy milk lowers blood pressure in men and women with mild to moderate essential hypertension, *J. Nutr. 132*, 1900−1902.
9. Jia, T.-L., Wang, H.-Z., Xie, L.-P., Wang, X.-Y., and Zhang, R.-Q. (2003) Daidzein enhances osteoblast growth that may be mediated by increased bone morphogenetic protein (BMP) production, *Biochem. Pharmacol. 65*, 709−715.
10. Skibola, C. F., and Smith, M. T. (2000) Potential health impacts of excessive flavonoid intake. *Free Radical Biol. Med. 29*, 375−383.
11. Messina, M. J., and Loprinzi, C. L. (2001) Soy for breast cancer survivors: a critical review of the literature, *J. Nutr. 131*, 3095S−3108S.
12. Newbold, R. R., Banks, E. P., Bullock, B., and Jefferson, W. N. (2001) Uterine adenocarcinoma in mice treated neonatally with genistein, *Cancer Res. 61*, 4325−4328.
13. Thigpen, J. E., Locklear, J., Haseman, J. K., Saunders, H., Grant, M. F., and Forsythe, D. B. (2001) Effects of the dietary phytoestrogens daidzein and genistein on the incidence of vulvar carcinomas in 129/J mice, *Cancer Detect. Prev. 25*, 527−532.
14. Allred, C. D., Allred, K. F., Ju, Y. H., Virant, S. M., and Helferich, W. G. (2001) Soy diets containing varying amounts of genistein stimulate growth of estrogen-dependent (MCF-7) tumors in a dose-dependent manner, *Cancer Res. 61*, 5045−5050.
15. Rao, C. V., Wang, C. X., Simi, B., Lubet, R., Kelloff, G., Steele, V., and Reddy, B. S. (1997) Enhancement of experimental colon cancer by genistein, *Cancer Res. 57*, 3717−3722.
16. McMichael-Phillips, D. F., Harding, C., Morton, M., Roberts, S. A., Howell, A., Potten, C. S., and Bundred, N. J. (1998) Effects of soy-protein supplementation on epithelial proliferation in the histologically normal human breast, *Am. J. Clin. Nutr. 68* (Suppl. 6), 1431S−1435S.
17. Petrakis, N. L., Barnes, S., King, E. B., Lowenstein, J., Wiencke, J., Lee, M. M., Miike, R., Kirk, M., and Coward, L. (1996) Stimulatory influence of soy protein isolate on breast secretion in pre- and postmenopausal women, *Cancer Epidemiol., Biomarkers Prev. 5*, 785−794.
18. Bernstein, L., and Ross, R. K. (1993) Endogenous hormones and breast cancer risk, *Epidemiol. Rev. 15*, 48−65.
19. IARC Working Group (1999) Hormonal contraception and postmenopausal hormonal therapy, in *IARC Monographs on the Evaluation of the Carcinogenic Risk of Chemicals to Humans*, Vol. 72, IARC, Lyon, France.
20. Nelson, H. D., Humphrey, L. L., Nygren, P., Teutsch, S. M., and Allan, J. D., (2002) Postmenopausal hormone replacement therapy: scientific review, *J. Am. Med. Assoc. 288*, 872−881.
21. Hiraku, Y., Yamashita, N., Nishiguchi, M., and Kawanishi, S. (2001) Catechol estrogens induce oxidative DNA damage and estradiol enhances cell proliferation, *Int. J. Cancer 92*, 333−337.
22. Lavigne, J. A., Goodman, J. E., Fonong, T., Odwin, S., He, P., Roberts, D. W., and Yager, J. D. (2001) The effects of catechol-O-methyltransferase inhibition on estrogen metabolite and oxidative DNA damage levels in estradiol-treated MCF-7 cells, *Cancer Res. 61*, 7488−7494.
23. Kulling, S. E., Honig, D. M., and Metzler, M. (2001) Oxidative metabolism of the soy isoflavones daidzein and genistein in humans in vitro and in vivo, *J. Agric. Food Chem. 49*, 3024−3033.
24. Roberts-Kirchhoff, E. S., Crowley, J. R., Hollenberg, P. F., and Kim, H. (1999) Metabolism of genistein by rat and human cytochrome P450s, *Chem. Res. Toxicol. 12*, 610−616.
25. Nishioka, H., Imoto, M., Sawa, T., Hamada, M., Naganawa, H., Takeuchi, T., and Umezawa, K. (1989) Screening of phosphatidylinositol kinase inhibitors from *Streptomyces*, *J. Antibiot. 42*, 823−825.
26. Soto, A. M., Sonnenschein, C., Chung, K. L., Fernandez, M. F., Olea, N., and Serrano, F. O. (1995) The E-SCREEN assay as a tool to identify estrogens: an update on estrogenic environmental pollutants, *Environ. Health Perspect. 103*, 113−122.
27. Lu, D., Kiriyama, Y., Lee, K. Y., and Giguere, V. (2001) Transcriptional regulation of the estrogen-inducible pS2 breast cancer marker gene by the ERR family of orphan nuclear receptors, *Cancer Res. 61*.
28. Rich, R. L., Hoth, L. R., Geoghegan, K. F., Brown, T. A., LeMotte, P. K., Simons, S. P., Hensley, P., and Myszka, D. G. (2002) Kinetic analysis of estrogen receptor/ligand interactions, *Proc. Natl. Acad. Sci. U.S.A. 99*, 8562−8567.
29. Murata, M., Moriya, K., Inoue, S., and Kawanishi, S. (1999) Oxidative damage to cellular and isolated DNA by metabolites of a fungicide *ortho*-phenylphenol, *Carcinogenesis 20*, 851−857.
30. Hiraku, Y., Murata, M., and Kawanishi, S. (2002) Determination of intracellular glutathione and thiols by high performance liquid chromatography with a gold electrode at the femtomole level: comparison with a spectroscopic assay, *Biochim. Biophys. Acta 1570*, 47−52.
31. Chumakov, P. (1990) EMBL Data Library, accession number X54156.
32. Murata, M., and Kawanishi, S. (2000) Oxidative DNA damage by vitamin A and its derivative via superoxide generation, *J. Biol. Chem. 275*, 2003−2008.
33. Capon, D. J., Chen, E. Y., Levinson, A. D., Seeburg, P. H., and Goeddel, D. V. (1983) Complete nucleotide sequences of the T24 human bladder carcinoma oncogene and its normal homologue, *Nature 302*, 33−37.
34. Yamamoto, K., and Kawanishi, S. (1989) Hydroxyl free radical is not the main active species in site-specific DNA damage induced by copper(II) ion and hydrogen peroxide, *J. Biol. Chem. 264*, 15435−15440.
35. Oikawa, S., and Kawanishi, S. (2000) Detection of DNA damage and analysis of its site-specificity, in *Experimental protocols for reactive oxygen and nitrogen species* (Taniguchi, N., and Gutterige, J. M. C., Eds.) pp 229−235, Oxford University Press, New York.
36. Maxam, A. M., and Gilbert, W. (1980) Sequencing end-labeled DNA with base-specific chemical cleavages, *Methods Enzymol. 65*, 499−560.
37. Malaisse, W. J., Hutton, J. C., Kawazu, S., Herchuelz, A., Valverde, I., and Sener, A. (1979) The stimulus-secretion coupling of glucose-induced insulin release. XXXV. The links between metabolic and cationic events, *Diabetologia 16*, 331−341.
38. Levine, A. J., Momand, J., and Finlay, C. A. (1991) The p53 tumor suppressor gene, *Nature 351*, 453−456.
39. Hartmann, A., Blaszyk, H., Saitoh, S., Tsushima, K., Tamura, Y., Cunningham, J. M., McGovern, R. M., Schroeder, J. J., Sommer, S. S., and Kovach, J. S. (1996) High frequency of p53 gene mutations in primary breast cancers in Japanese women, a low-incidence population, *Br. J. Cancer 73*, 896−901.
40. Wang, T. T., Sathyamoorthy, N., and Phang, J. M. (1996) Molecular effects of genistein on estrogen receptor mediated pathways, *Carcinogenesis 17*, 271−275.

41. Hsieh, C. Y., Santell, R. C., Haslam, S. Z., and Helferich, W. G. (1998) Estrogenic effects of genistein on the growth of estrogen receptor-positive human breast cancer (MCF-7) cells in vitro and in vivo, *Cancer Res. 58*, 3833−3838.
42. Cheskis, B. J., Karathanasis, S., and Lyttle, C. R. (1997) Estrogen receptor ligands modulate its interaction with DNA, *J. Biol. Chem. 272*, 11384−11391.
43. Breinholt, V., and Larsen, J. C. (1998) Detection of weak estrogenic flavonoids using a recombinant yeast strain and a modified MCF7 cell proliferation assay, *Chem. Res. Toxicol. 11*, 622−629.
44. Kuiper, G. G., Lemmen, J. G., Carlsson, B., Corton, J. C., Safe, S. H., van der Saag, P. T., van der Burg, B., and Gustafsson, J. A. (1998) Interaction of estrogenic chemicals and phytoestrogens with estrogen receptor β, *Endocrinology 139*, 4252−4263.
45. Nikov, G. N., Hopkins, N. E., Boue, S., and Alworth, W. L. (2000) Interactions of dietary estrogens with human estrogen receptors and the effect on estrogen receptor-estrogen response element complex formation, *Environ. Health Perspect. 108*, 867−872.
46. Wong, C. W., Komm, B., and Cheskis, B. J. (2001) Structure−function evaluation of ER α and β interplay with SRC family coactivators. ER selective ligands, *Biochemistry 40*, 6756−6765.
47. Tsutsui, T., and Barrett, J. C. (1997) Neoplastic transformation of cultured mammalian cells by estrogens and estrogen-like chemicals, *Environ. Health Perspect. 105* (Suppl. 3), 619−624.
48. Liehr, J. G. (2001) Genotoxicity of the steroidal oestrogens oestrone and oestradiol: possible mechanism of uterine and mammary cancer development, *Hum. Reproduct. Update 7*, 273−281.
49. van Duursen, M. B., Sanderson, J. T., van der Bruggen, M., van der Linden, J., and van den Berg, M. (2003) Effects of several dioxin-like compounds on estrogen metabolism in the malignant MCF-7 and nontumorigenic MCF-10A human mammary epithelial cell lines, *Toxicol. Appl. Pharmacol. 190*, 241−250.
50. Price, R. J., Surry, D., Renwick, A. B., Meneses-Lorente, G., Lake, B. G., and Evans, D. C. (2000) CYP isoform induction screening in 96-well plates: use of 7-benzyloxy-4-trifluoromethylcoumarin as a substrate for studies with rat hepatocytes, *Xenobiotica 30*, 781−795.
51. Pryor, W. A., and Tang, R. H. (1978) Ethylene formation from methional, *Biochem. Biophys. Res. Commun. 81*, 498−503.
52. Nakai, N., Murata, M., Nagahama, M., Hirase, T., Tanaka, M., Fujikawa, T., Nakao, N., Nakashima, K., and Kawanishi, S. (2003) Oxidative DNA damage induced by toluene is involved in its male reproductive toxicity, *Free Radical Res. 37*, 69−76.
53. Oikawa, S., Hirosawa, I., Hirakawa, K., and Kawanishi, S. (2001) Site specificity and mechanism of oxidative DNA damage induced by carcinogenic catechol, *Carcinogenesis 22*, 1239−1245.
54. Hussain, S. P., Hofseth, L. J., and Harris, C. C. (2003) Radical causes of cancer, *Nat. Rev. Cancer 3*, 276−285.
55. Perquin, M., Oster, T., Maul, A., Froment, N., Untereiner, M., and Bagrel, D. (2000) The glutathione-related detoxification pathway in the human breast: a highly coordinated system disrupted in the tumour tissues, *Cancer Lett. 158*, 7−16.
56. Musarrat, J., Arezina-Wilson, J., and Wani, A. A. (1996) Prognostic and aetiological relevance of 8-hydroxyguanosine in human breast carcinogenesis, *Eur. J. Cancer 32*, 1209−1214.
57. Li, D., Zhang, W., Zhu, J., Chang, P., Sahin, A., Singletary, E., Bondy, M., Hazra, T., Mitra, S., Lau, S. S., Shen, J., and DiGiovanni, J. (2001) Oxidative DNA damage and 8-hydroxy-2′-deoxyguanosine DNA glycosylase/apurinic lyase in human breast cancer, *Mol. Carcinog. 31*, 214−223.

BI035613D

Free Radical Research, Volume 38 Number 5 (May 2004), pp. 439–447

Taylor & Francis
healthsciences

Photo-irradiated Titanium Dioxide Catalyzes Site Specific DNA Damage via Generation of Hydrogen Peroxide

KAZUTAKA HIRAKAWA[a], MASAFUMI MORI[b], MAMI YOSHIDA[a], SHINJI OIKAWA[b] and SHOSUKE KAWANISHI[b,*]

[a]*Department of Radiation Chemistry, Life Science Research Center, Mie University, Edobashi 2-174, Tsu Mie 514-8507, Japan;* [b]*Department of Environmental and Molecular Medicine, Mie University School of Medicine, Edobashi 2-174, Tsu Mie 514-8507, Japan*

Accepted by Professor J. Cadet

(Received 2 September 2003; In revised form 21 January 2004)

Titanium dioxide (TiO_2) is a potential photosensitizer for photodynamic therapy. In this study, the mechanism of DNA damage catalyzed by photo-irradiated TiO_2 was examined using [^{32}P]-5′-end-labeled DNA fragments obtained from human genes. Photo-irradiated TiO_2 (anatase and rutile) caused DNA cleavage frequently at the guanine residue in the presence of Cu(II) after *E. coli* formamidopyrimidine-DNA glycosylase treatment, and the thymine residue was also cleaved after piperidine treatment. Catalase, SOD and bathocuproine, a chelator of Cu(I), inhibited the DNA damage, suggesting the involvement of hydrogen peroxide, superoxide and Cu(I). The photocatalytic generation of Cu(I) from Cu(II) was decreased by the addition of SOD. These findings suggest that the inhibitory effect of SOD on DNA damage is due to the inhibition of the reduction of Cu(II) by superoxide. We also measured the formation of 8-oxo-7,8-dihydro-2′-deoxyguanosine, an indicator of oxidative DNA damage, and showed that anatase is more active than rutile. On the other hand, high concentration of anatase caused DNA damage in the absence of Cu(II). Typical free hydroxyl radical scavengers, such as ethanol, mannnitol, sodium formate and DMSO, inhibited the copper-independent DNA photodamage by anatase. In conclusion, photo-irradiated TiO_2 particles catalyze the copper-mediated site-specific DNA damage via the formation of hydrogen peroxide rather than that of a free hydroxyl radical. This DNA-damaging mechanism may participate in the photo-toxicity of TiO_2.

Keywords: Titanium dioxide; Oxidative DNA damage; Superoxide; Hydrogen peroxide; Copper; Free hydroxyl radicals

Abbreviations: TiO_2, titanium dioxide; ROS, reactive oxygen species; $O_2^{\cdot-}$, superoxide anion radical; H_2O_2, hydrogen peroxide; $^{\cdot}OH$, free hydroxyl radical; PDT, photodynamic therapy; 8-oxodGuo, 8-oxo-7,8-dihydro-2′-deoxyguanosine; dGuo, 2′-deoxyguanosine; HPLC-ECD, high-performance liquid chromatography equipped with an electrochemical detector; DTPA, diethylenetriamine-*N,N,N′,N″,N″*-pentaacetic acid; Fpg, *E.coli* formamidopyrimidine-DNA glycosylase

INTRODUCTION

Titanium dioxide (TiO_2) is a well-known photocatalyst.[1] The crystalline forms of TiO_2, anatase and rutile, are semiconductors with band gap energies of 3.26 and 3.06 eV, respectively. TiO_2 absorbs UVA light, catalyzing the generation of reactive oxygen species (ROS), such as superoxide anion radical ($O_2^{\cdot-}$), hydrogen peroxide (H_2O_2), free hydroxyl radical ($^{\cdot}OH$), and singlet oxygen, in aqueous media.[1–3] Photo-irradiated TiO_2 demonstrates bactericidal effects and is widely used for photocatalytic sterilization.[1,4–6] Recently, the application of TiO_2 as a photosensitizer of photodynamic therapy (PDT) was proposed.[1,7–10] PDT is a relatively new treatment for certain types of cancer, including endobronchial and esophageal cancers.[11] TiO_2 particles can be incorporated into cells[7,12] and kill cancer cells during UVA irradiation.[1,7–10,12] The inhibitory effect of tumor growth by photo-irradiated TiO_2 was also reported in an animal experiment using mice.[1,10] The mechanism of cytotoxicity by photocatalysis of TiO_2 is accompanied by cell membrane damage.[13] In addition, TiO_2 induces photodamage to DNA in human cells,[14] mouse lymphoma cells,[15] and phage.[16] However, the mechanism underlying

*Corresponding author. Tel.: +81-59-231-5011. Fax: +81-59-231-5011. E-mail: kawanisi@doc.medic.mie-u.ac.jp

ISSN 1071-5762 print/ISSN 1029-2470 online © 2004 Taylor & Francis Ltd
DOI: 10.1080/1071576042000206487

DNA damage photocatalyzed by TiO_2 is not well understood.

In this study, the mechanism and the site specificity of DNA damage by photo-irradiated TiO_2 (anatase and rutitle) were examined using a ^{32}P-5′-end-labeled DNA fragment obtained from the human *p53* and *p16* tumor suppressor genes and the c-Ha-*ras*-1 protooncogene. The formation of 8-oxo-7,8-dihydro-2′-deoxyguanosine (8-oxodGuo), an oxidation product of 2′-deoxyguanosine (dGuo), was also measured using an electrochemical detector coupled to high-performance liquid chromatography (HPCL-ECD).

MATERIALS AND METHODS

Materials

TiO_2 particles (anatase and rutile) with an average size of 50–300 nm in diameter were purchased from Kanto Chemical Co. (Tokyo, Japan). The particles were ultra-sonically dispersed in water. Restriction enzymes (*Ava*I and *Pst*I) and T_4 polynucleotide kinase were purchased from New England Biolabs (Beverly, MA). Restriction enzymes (*Apa*I, *BssH*II, *EcoR*I, *Mro*I and *Xba*I) and calf intestine phosphatase were from Boehringer Mannheim GmbH (Mannheim, Germany). [γ-^{32}P]-ATP was from New England Nuclear (Boston, MA). Diethylenetriamine-*N,N,N′,N″,N‴*-pentaacetic acid (DTPA) and bathocuproinedisulfonic acid were from Dojin Chemicals Co. (Kumamoto, Japan). SOD (3000 units/mg from bovine erythrocytes) and catalase (45,000 units/mg from bovine liver) were from Sigma Chemical Co. (St Louis, MO). Methional (3-methylthiopropionaldehyde) was from Tokyo Kaksei (Tokyo, Japan). DMSO was from Aldrich Chemical Co. (Milwaukee, WI). Copper(II) chloride dihydrate was from Nacalai Tesque, Inc. (Kyoto, Japan). *E. coli* formamidopyrimidine-DNA glycosylase (Fpg) was from Trevigen Co. (Gaithersburg, MD).

Preparation of ^{32}P-5′-end-labeled DNA Fragments

DNA fragments were obtained from the human *p53*[17] and *p16*[18] tumor suppressor genes and the c-Ha-*ras*-1 protooncogene.[19] The DNA fragment of the *p53* tumor suppressor gene was prepared from pUC18 plasmid, ligated fragments containing exons of *p53* gene. A singly ^{32}P-5′-end-labeled double-stranded 443-bp fragment (*Apa*I 14179-*EcoR*I*14621) and a 211-bp fragment (*Hind*III* 13972-*Apa*I 14182) were prepared according to the method described previously.[20] Exon-containing DNA fragments were also obtained from the human *p16* tumor suppressor gene; these fragments were subcloned into the Pgem-T Easy Vector (Promega Corp. Madison, WI). A singly labeled 324 bp DNA fragment (*EcoR*I* 9466-*BssH*II 9789) and a 158-bp fragment (*Mro*I 6173-*Eco*RI* 6330) were prepared as described previously.[21] The DNA fragment of the c-Ha-*ras*-1 protooncogene was prepared from plasmid pbcNI, which carries a 6.6 kb *Bam*HI chromosomal DNA segment containing the c-Ha-*ras*-1 gene. A singly labeled 337 bp fragment (*Pst*I 2345-*Ava*I* 2681) and a 261-bp fragment (*Ava*I* 1645-*Xba*I 1905) were obtained according to a method described previously.[22] Nucleotide numbering starts with the *Bam*HI site.[19] The asterisk indicates the ^{32}P labeling.

Detection of Damage to Isolated DNA by Photo-irradiated TiO_2

The standard reaction mixture in a microtube (1.5 ml Eppendorf) contained the ^{32}P-DNA fragment (<1 μM) and 20 μM calf thymus DNA, indicated amounts of TiO_2, and 5 μM DTPA in a 10 mM sodium phosphate buffer (pH 7.8). DTPA was used to remove the contaminated metal ions. To clarify the effect of metal ions on DNA photodamage, a 20 μM metal ion, such as $CuCl_2$ was used. The mixtures were exposed to 10 J/cm^2 UVA light using 10-W UV lamp (λ_{max} = 365 nm, 1.4 mW/cm^2) (UVP Inc., CA). Subsequently, the DNA was treated with 1 M piperidine for 20 min at 90°C or 10 units of Fpg in the reaction buffer (10 mM HEPES-KOH (pH 7.4), 100 mM KCl, 10 mM EDTA and 0.1 mg/ml BSA) for 2 h at 37°C. The DNA fragments were subjected to electrophoresis on an 8 M urea/8% polyacrylamide gel. The autoradiogram was obtained by exposing an X-ray film to the gel. The preferred cleavage sites were determined by direct comparison of the positions of the oligonucleotides with those produced by the chemical reactions of the Maxam–Gilbert procedure[23] using a DNA-sequencing system (LKB 2010 Macrophor, Pharmacia Biotech, Uppsala, Sweden). A relative amount of DNA fragments was measured by scanning the autoradiogram with a laser densitometer (LKB 2222 UltroScan XL, Pharmacia Biotech).

Measurement of 8-OxodGuo Formation in Calf Thymus DNA by Photo-irradiated TiO_2

Formation of 8-oxodGuo was measured by a modification of a reported method.[24] The reaction mixture in a tube (1.5 ml Eppendorf) contained indicated concentration of TiO_2 (anatase or rutile), 20 μM $CuCl_2$, 100 μM/base calf thymus DNA and 5 μM DTPA in 100 μl of 4 mM sodium phosphate buffer (pH 7.8). The mixtures were exposed to 10 J/cm^2 UVA light using 10-W UV lamp (λ_{max} = 365 nm, 1.4 mW/cm^2). After ethanol precipitation, DNA was digested to the nucleosides with nuclease P_1 and calf intestine phosphatase,

and analyzed with an HPLC-ECD, as described previously.[25]

UV–visible Spectra Measurements on Cu(II) Reduction Photocatalyzed by TiO_2

UV–visible spectra for the reduction of Cu(II) to Cu(I) by photo-irradiated TiO_2 were measured with a UV–visible spectrometer (UV-2500PC, Shimadzu, Kyoto, Japan) using bathocuproine as a Cu(I)-chelator. The standard reaction mixture contained 8 μg/ml TiO_2, 20 μM $CuCl_2$ and 10 μM bathocuproine in 1 ml of 10 mM sodium phosphate buffer (pH 7.8). The mixtures were exposed to 2 J/cm^2 UVA light using 10-W UV lamp (λ_{max} = 365 nm, 1.4 mW/cm^2). After irradiation, TiO_2 particles were removed by centrifugation and the absorption maximum at 480 nm of the Cu(I)-bathocuproine complex[26] was measured.

RESULTS

DNA Damage by Photo-irradiated TiO_2

Photo-irradiated TiO_2 particles (anatase and rutile) caused DNA damage in the presence of Cu(II) (Fig. 1). Mn(II), Fe(III), Co(II) and Ni(II) did not mediate DNA damage (data not shown). Even without piperidine treatment, oligonucleotides were slightly formed by photo-irradiated TiO_2 (data not shown), indicating the breakage of the deoxyribose phosphate backbone. The extent of DNA damage was increased by piperidine treatment, suggesting that base modifications were also induced by photo-irradiated TiO_2 in the presence of Cu(II). Without irradiation, TiO_2 showed no damage to DNA (Fig. 1). DNA damage induced by anatase was stronger than that by rutile.

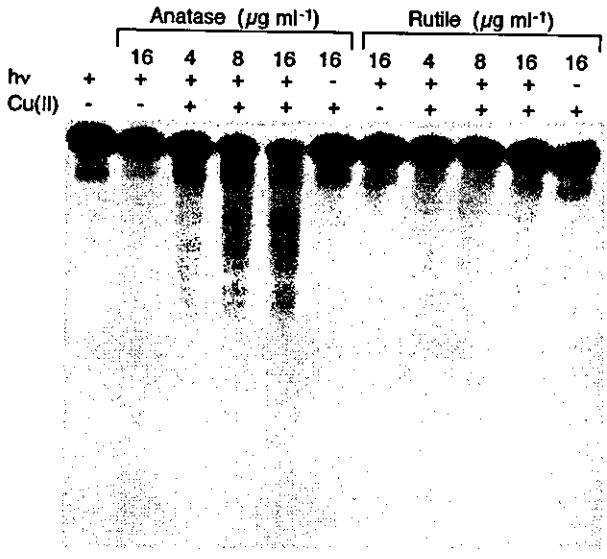

FIGURE 1 Autoradiogram of ^{32}P-labeled DNA fragment irradiated with UVA light in the presence of TiO_2. The reaction mixtures contained the ^{32}P-5′-end-labeled 158 bp DNA fragment, 20 μM/base calf thymus DNA, the indicated concentrations of TiO_2, 20 μM $CuCl_2$, and 5 μM DTPA in 100 μl of 10 mM sodium phosphate buffer (pH 7.8). The reaction mixtures were irradiated with UVA light (λ_{max} = 365 nm, 10 J/cm^2). Then, the DNA fragments were treated with 1 M piperidine for 20 min at 90°C and electrophoresed on an 8% polyacrylamide/8M urea gel.

Effects of Scavengers and Bathocuproine on DNA Damage by Photo-irradiated TiO_2

To investigate the identity of the reactive species involved in DNA damage, we evaluated the inhibitory effects of scavengers of ROS and bathocuproine, a chelator of Cu(I), on DNA damage (Fig. 2).

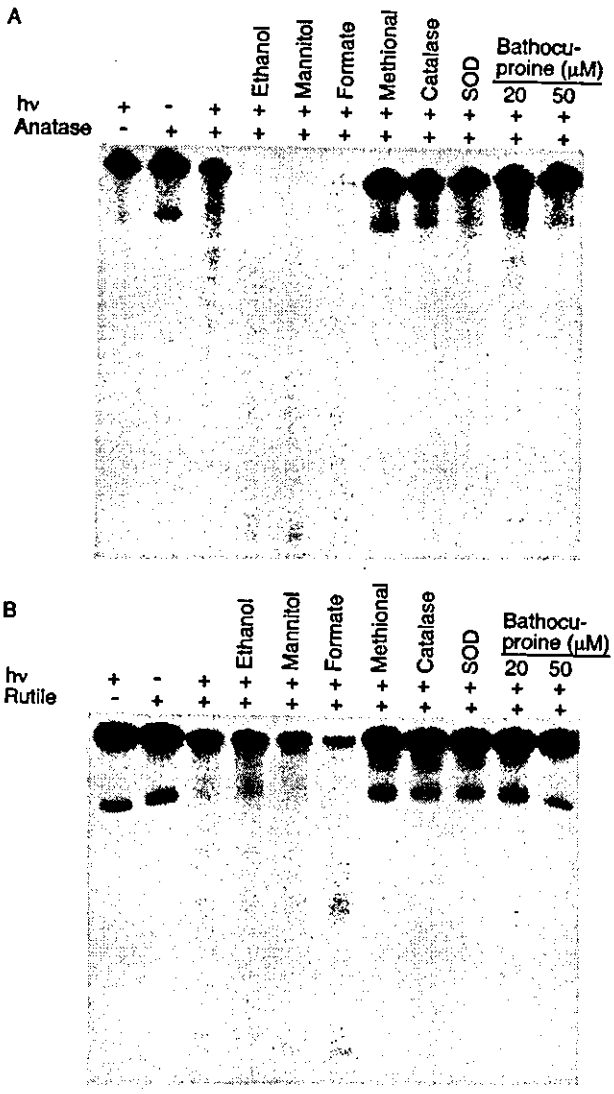

FIGURE 2 Effects of scavengers on DNA damage induced by photo-irradiated TiO_2 in the presence of Cu(II). The reaction mixtures contained the ^{32}P-5′-end-labeled 261 bp (A) or 443 bp (B) DNA fragment, 20 μM/base calf thymus DNA, 20 μM $CuCl_2$, 5 μM DTPA and 8 μg/ml anatase (A) or 8 μg/ml rutile (B) in 100 μl of 10 mM sodium phosphate buffer (pH 7.8). The reaction mixtures were irradiated with UVA light (λ_{max} = 365 nm, 10 J/cm^2) and treated as described in the legend to Fig. 1. The concentrations of scavengers and bathocuproine were as follows: 5v% ethanol, 0.1 M mannitol, 0.1 M sodium formate, 0.1 M methional, 30 units of SOD and 50 units of catalase.

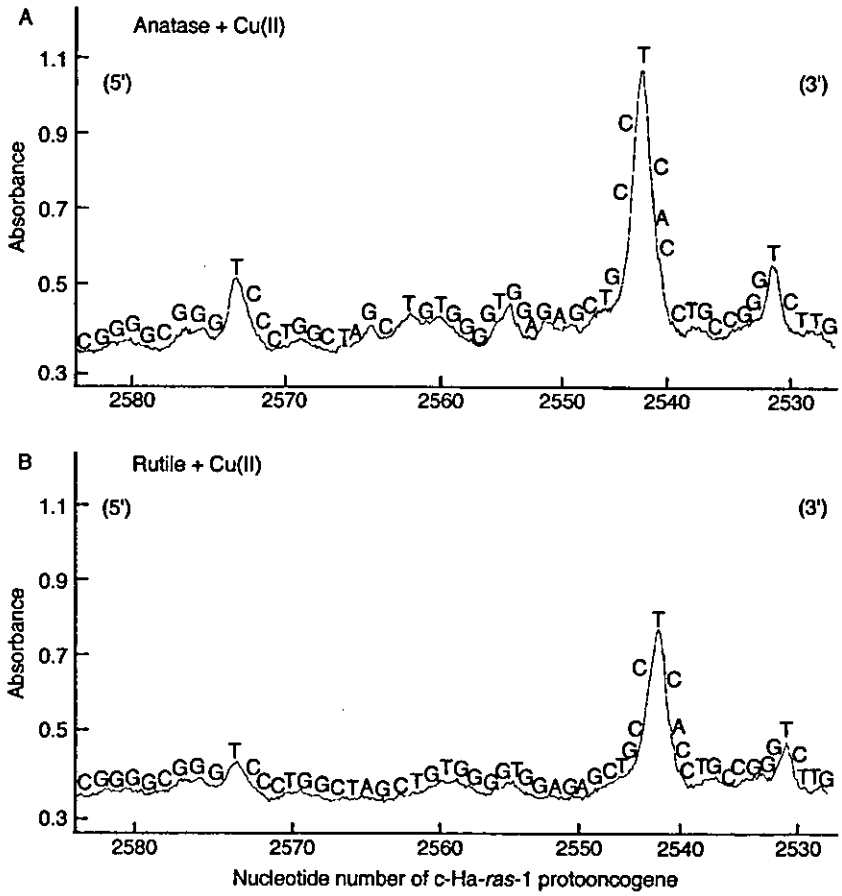

FIGURE 3 Site specificity of DNA damage induced by photo-irradiated TiO_2 in the presence of Cu(II). The reaction mixtures contained the ^{32}P-5′-end-labeled 337 bp DNA fragment (c-Ha-*ras*-1 protooncogene), 20 μM/base calf thymus DNA, 20 μM $CuCl_2$, 5 μM DTPA and 8 μg/ml anatase (A) or 8 μg/ml rutile (B) in 100 μl of 10 mM sodium phosphate buffer (pH 7.8). Mixtures were irradiated with UVA light (λ_{max} = 365 nm, 10 J/cm^2). The DNA fragments were then treated with piperidine. Subsequently, the DNA was analyzed and the relative amounts of oligonucleotides were measured by the methods described in the "Materials and methods section". The horizontal axis shows the nucleotide number of the human c-Ha-*ras*-1 protooncogene.

DNA damage induced by photo-irradiated anatase plus Cu(II) was significantly inhibited by catalase, SOD and bathocuproine (Fig. 2A). Similar scavenging effects were observed in the case of rutile plus Cu(II) (Fig. 2B). These results suggest the involvement of H_2O_2, $O_2^{\cdot-}$, and Cu(I). Methional also inhibited DNA damage. Typical $^{\cdot}OH$ scavengers, such as ethanol, mannitol and sodium formate, could not inhibit DNA damage. Addition of ethanol, mannitol and sodium formate enhanced DNA photodamage by anatase plus Cu(II) (Fig. 2A).

Site Specificity of DNA Damage by Photo-irradiated TiO_2

The patterns of DNA damage induced by photo-irradiated anatase was quite similar to that induced by rutile (Fig. 3A and B). Photo-irradiated TiO_2 particles formed piperidine-labile products at the underlined bases of 5′-TC (Figs. 3 and 4A) and 5′-TG (Fig. 4A) in the presence of Cu(II). With Fpg treatment, the DNA cleavage occurred frequently at the underlined guanine residue of 5′-TG, another guanine and cytosine (Fig. 4B). Fpg mainly catalyzes the excision of piperidine-resistant 8-oxodGuo, an oxidative product of dGuo.[27] Fpg also mediates the cleavages of the oxidative cytosine, such as 5-hydroxycytosine.[28]

Formation of 8-OxodGuo in Calf Thymus DNA by Photo-irradiated TiO_2

Photo-irradiated anatase and rutile induced 8-oxodGuo formation in the presence of Cu(II) (Fig. 5). The formation of 8-oxodGuo by photo-irradiated anatase was increased in a dose-dependent manner, whereas that by rutile plateaued when more than 4 μg/ml TiO_2 was used. A comparison of 8-oxodGuo formation by anatase and rutile suggested that the DNA-damaging ability of anatase is stronger than that of rutile.

Reduction of Cu(II) by Photo-irradiated TiO_2

After photo-irradiation of the mixture including TiO_2, Cu(II) and bathocuproine, a typical absorption spectrum of Cu(I)-bathocuproine complex[26] with

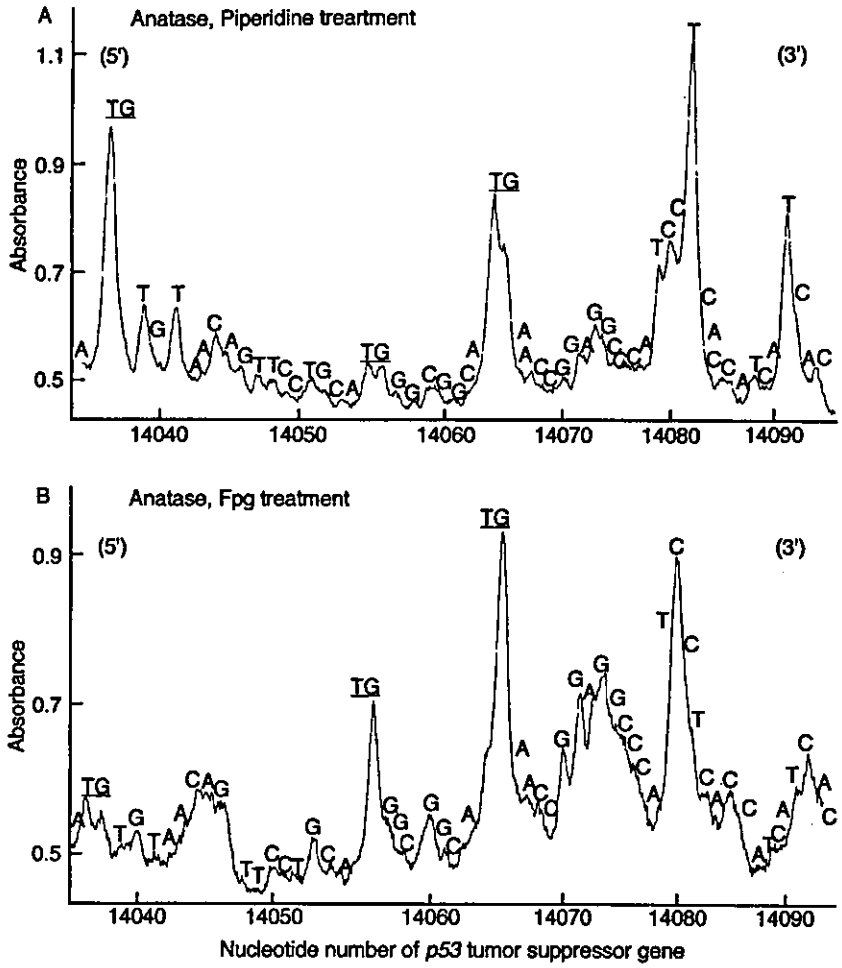

FIGURE 4 Site specificity of DNA damage induced by photo-irradiated anatase. The reaction mixtures contained the ^{32}P-5'-end-labeled 211 bp DNA fragment (*p53* tumor suppressor gene), 20 μM/base calf thymus DNA, 5 μM DTPA, 20 μM $CuCl_2$ and 8 μg/ml anatase in 100 μl of 10 mM sodium phosphate buffer (pH 7.8). Mixtures were irradiated with UVA light (λ_{max} = 365 nm, 10 J/cm^2). Subsequently, the DNA fragments were treated with piperidine (A) or Fpg (B). The DNA was analyzed and the relative amounts of oligonucleotides were measured by the methods described in the Materials and methods section. The horizontal axis shows the nucleotide numbers of the *p53* tumor suppressor gene.

the maximum at 480 nm was observed and increased depending on the concentration of TiO_2 (Fig. 6), indicating the reduction of Cu(II) to Cu(I) by the photocatalysis of TiO_2. The formation of the Cu(I)-bathocuproine complex was decreased by SOD, suggesting the Cu(II) reduction by $O_2^{\cdot-}$. SOD did not completely inhibit Cu(I) generation because Cu(II) can be easily reduced in the presence of bathocuproine. The formation of the Cu(I)-bathocuproine complex was accelerated under argon (data not shown), indicating that Cu(II) can be directly reduced by the electron formed in the conductive band of TiO_2 in the absence of molecular oxygen.

DNA Photodamage by a High Concentration of Anatase in the Absence of Cu(II)

A high concentration of anatase caused DNA damage in the absence of Cu(II). No metal-independent DNA photodamage was detected when rutile was used, but as the DNA targets employed were relatively short and therefore, cannot detect rare damage this dose not imply that rutile is incapable of inflicting metal-independent photodamage on DNA. DNA photodamage induced by a high concentration of anatase was inhibited by $^{\cdot}OH$ scavengers and methional (Fig. 7), suggesting the involvement of $^{\cdot}OH$. A high concentration of anatase induced piperidine-labile sites at every nucleobase in the absence of Cu(II) (Fig. 8). This cleavage pattern is quite different from the Cu(II)-dependent DNA photodamage by anatase.

DISCUSSION

The present study has demonstrated that photo-irradiated TiO_2 particles catalyze DNA damage in the presence of Cu(II). DNA damage induced by anatase was stronger than that by rutile. The DNA damage was enhanced by piperidine treatment, suggesting that photo-irradiated TiO_2 caused not only DNA strand breakage but also base

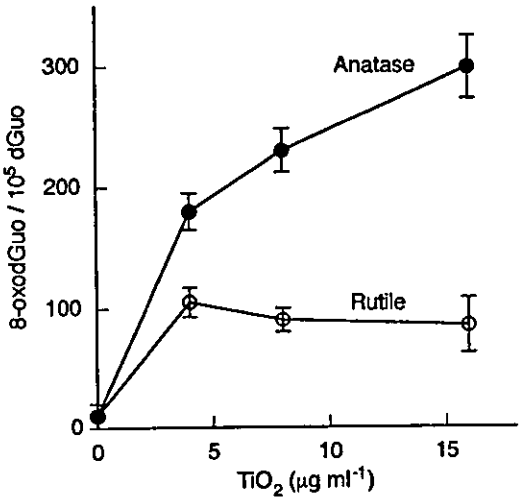

FIGURE 5 Formation of 8-oxodGuo induced by photo-irradiated TiO_2 in the presence of Cu(II). The reaction mixtures contained 100 μM/base calf thymus DNA, TiO_2, 20 μM $CuCl_2$ and 5 μM DTPA in 100 μl of 4 mM sodium phosphate buffer (pH 7.8). After photo-irradiation (λ_{max} = 365 nm, 10 J/cm^2), DNA fragment was enzymatically digested into nucleosides, and 8-oxodGuo formation was measured with an HPLC-ECD as described in the Materials and methods section.

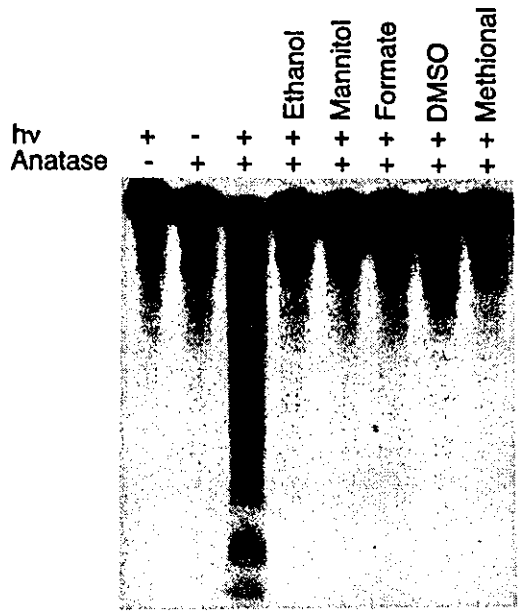

FIGURE 7 Effects of hydroxyl radical scavengers on DNA damage induced by photo-irradiated anatase. The reaction mixtures contained the ^{32}P-5′-end-labeled 324 bp DNA fragment 20 μM/base calf thymus DNA, 5 μM DTPA and 80 μg/ml anatase in 100 μl of 10 mM sodium phosphate buffer (pH 7.8). The reaction mixtures were irradiated with UVA light (λ_{max} = 365 nm, 10 J/cm^2) and treated as described in the legend of Fig. 1. The concentrations of scavengers were as follows: 5 v% ethanol, 0.1 M mannitol, 0.1 M sodium formate, 5 v% DMSO and 0.1 M methional.

modification. Photo-irradiated TiO_2 formed piperidine-labile lesions at the underlined bases of 5′-TG and 5′-TC. Furthermore, TiO_2 caused DNA photocleavage at the underlined guanine of 5′-TG and the cytosine residues in a DNA fragment treated with Fpg, which catalyzes the excision of piperidine-resistant 8-oxodGuo.[27] Fpg also mediated the cleavages of the oxidative products of cytosine, such as 5-hydroxycytosine.[28] The present study suggests that photo-irradiated TiO_2 induces 8-oxodGuo formation adjacent to piperidine-labile thymine lesions. Although the present method based on Maxam–Gilbert procedure dose not clearly show double-base damage on the same DNA molecule, the data from the DNA cleavage pattern stochastically suggest the involvement of a double-base lesion. It has been appropriately postulated that double-base lesions can be generated from one radical hit that leads through a secondary reaction to a tandem base modification at pyrimidine and the adjacent residues.[29–31] Indeed, tandem mutations in human cells can be induced by H_2O_2 plus Cu(II) via vicinal or cross-linked base damage.[32]

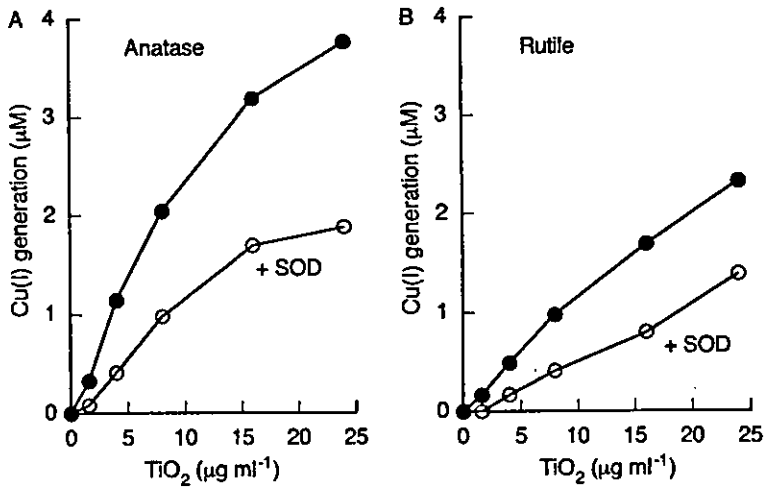

FIGURE 6 Reduction of Cu(II) by photo-irradiated TiO_2. The reaction mixtures contained 20 μM $CuCl_2$, TiO_2 and 10 μM bathocuproine in 1 ml of 10 mM sodium phosphate buffer (pH 7.8). After photo-irradiation (λ_{max} = 365 nm, 2 J/cm^2), the concentration of formed Cu(I)-bathocuproine complex was determined by measurement of absorbance at 480 nm.

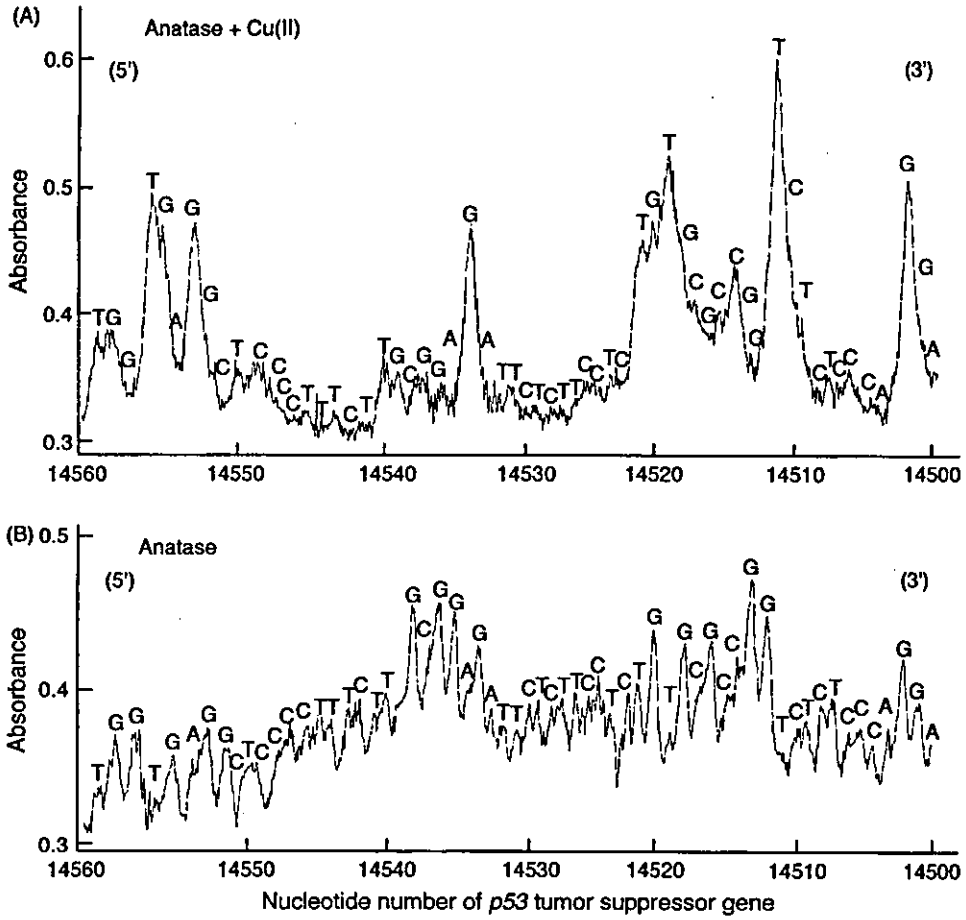

FIGURE 8 Site specificity of DNA damage induced by photo-irradiated anatase. The reaction mixtures contained the ^{32}P-5'-end-labeled 443bp DNA fragment (*p53* tumor suppressor gene), 20 μM/base calf thymus DNA, 5 μM DTPA and 8 μg/ml anatase with 20 μM $CuCl_2$ (A) or 80 μg/ml anatase without $CuCl_2$ (B) in 100 μl of 10 mM sodium phosphate buffer (pH 7.8). Mixtures were irradiated with UVA light (λ_{max} = 365 nm, 10 J/cm^2). Subsequently, the DNA fragments were treated with piperidine. The DNA was analyzed and the relative amounts of oligonucleotides were measured by the methods described in the Materials and methods section. The horizontal axis shows the nucleotide numbers of the *p53* tumor suppressor gene.

Since cluster damage in living cells is poorly repaired,[33] such clustered damage, including double-base lesions, appears to play an important role in the phototoxicity of TiO_2.

The effects of ROS scavengers and bathocuproine on DNA damage suggest the participation of H_2O_2 and Cu(I). Typical ·OH scavengers showed no or little inhibitory effects on DNA damage, although the possibility of DNA damage by *in situ*-produced ·OH cannot be ignored. The inhibitory effect of methional on DNA damage can be explained by the assumption that sulfur compounds scavenge less reactive species than ·OH.[34] It has also been reported that ·OH is not the main reactive species involved in DNA damage by H_2O_2 and Cu(I).[22,31] DNA-associated Cu(I) ions may generate other oxidants, including a copper-peroxo intermediate, such as Cu(I)-OOH, which is generated from the reaction of H_2O_2 and Cu(I).[35,36] The generation of these reactive species should be involved in the formation of piperidine-labile products and 8-oxodGuo. On the other hand, a high concentration of anatase could induce DNA photodamage in the absence of Cu(II). The effects of typical ·OH scavengers on DNA damage suggest the involvement of ·OH. The DNA damage induced by photo-irradiated anatase without Cu(II) was observed at every nucleotides with little site specificity, supporting the contribution of ·OH to DNA damage.[35]

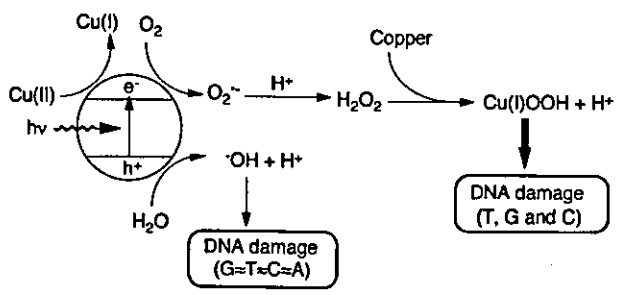

FIGURE 9 Proposed mechanism of DNA damage induced by photo-irradiated TiO_2.

A possible mechanism of DNA damage induced by photo-irradiated TiO_2 is shown in Fig. 9. The crystalline forms of TiO_2, anatase and rutile, are semiconductors with band gap energies of 3.26 and

3.06 eV, corresponding to light of 385 and 400 nm, respectively. When a TiO_2 semiconductor absorbs light with energy greater than its band gap, electrons in the valence band are excited to the conduction band, creating electron-hole pairs and causing various chemical reactions.[1] The electron (e^-) is a reducing agent, whereas the hole (h^+) is a powerful oxidizing agent. In aqueous environments, the electron reduces oxygen to give $O_2^{\cdot-}$, and the hole oxidizes a water molecule to yield $^{\cdot}OH$. Formed $O_2^{\cdot-}$ can be dismutated into H_2O_2. The experimental results of the formation of the Cu(I)-bathocuproine complex suggest that oxygen reduction precedes the Cu(II) reduction in the photocatalytic reaction of TiO_2 under aerobic condition, since the concentration of dissolved oxygen is much higher than that of Cu(II). The Cu(I) generation can be mediated by $O_2^{\cdot-}$. H_2O_2 reacts with Cu(I) to generate other oxidants, including a copper-peroxo intermediate, resulting in the oxidation of nucleobases. Copper, which is an essential component of chromatin,[37,38] is found to bind DNA with high affinity.[39,40] Therefore, copper may play an important role in ROS generation *in vivo*, although mammals have evolved means of minimizing the levels of free copper ions and most copper ions bind to protein carriers and transporters.[41] $^{\cdot}OH$ formed by the reaction of water with a hole in the valence band of TiO_2 also slightly participates in DNA damage by anatase. Because $^{\cdot}OH$ is strong oxidant, $^{\cdot}OH$ can damage every nucleobase.[35] This study suggested that H_2O_2 mainly participates in the phototoxicity of TiO_2 and that the contribution of $^{\cdot}OH$ is small. Quite appropriately, Fujishima *et al.* reported the involvement of peroxide generated from $O_2^{\cdot-}$ in the cytotoxicity of illuminated TiO_2.[1] These findings were also supported by the relatively small quantum yield of $^{\cdot}OH$ generation[42] in TiO_2 photocatalysis.

TiO_2 is a potential photosensitizer for PDT.[1,7–10] TiO_2 particles can be incorporated into cancer cells and demonstrate cytotoxicity under photo-irradiation.[1,7–10,12] Photo-irradiated TiO_2 catalyzes a number of functional changes in cells including altered permeability of cellular membranes to potassium and calcium ions, release of RNA and proteins and cytotoxicity.[13] It has also been reported that DNA can be a target molecule of the photocatalysis of TiO_2 *in vivo*.[14–16] The present study has shown that, under photo-irradiation, TiO_2 particles mainly caused copper-dependent DNA damage through H_2O_2 generation *in vitro*. Other metal ions may play an important role in the phototoxicity of TiO_2 *in vivo*. Although TiO_2 is not likely to be incorporated in a cell nucleus, H_2O_2 generated via a photocatalytic reaction can be easily diffused and incorporated in a cell nucleus, leading to DNA damage. Several studies have demonstrated that DNA can be an alternative potential target of PDT.[43,44] Therefore, the metal-mediated DNA damage through the photocatalysis of TiO_2 may participate in cytotoxicity by photo-irradiated TiO_2.

Acknowledgements

This work was supported by a Grant-in-Aid for Scientific Research on Priority Areas (417) from the Ministry of Education, Culture, Sports, Science and Technology (MEXT) of the Japanese Government.

References

[1] Fujishima, A., Rao, T.N. and Tryk, D.A. (2000) "Titanium dioxide photoatalysis", *J. Photochem. Photobiol. C Photochem. Rev.* **1**, 1–21.
[2] Konaka, R., Kasahara, E., Dunlap, W.C., Yamamoto, Y., Chien, K.C. and Inoue, M. (1999) "Irradiation of titanium dioxide generates both singlet oxygen and superoxide anion", *Free Radic. Biol. Med.* **27**, 294–300.
[3] Konaka, R., Kasahara, E., Dunlap, W.C., Yamamoto, Y., Chien, K.C. and Inoue, M. (2001) "Ultraviolet irradiation of titanium dioxide in aqueous dispersion generates singlet oxygen", *Redox Rep.* **6**, 319–325.
[4] Kikuchi, Y., Sunada, K., Iyoda, T., Hashimoto, K. and Fujishima, A. (1997) "Photocatalytic bactericidal effect of TiO_2 thin films: dynamic view of the active oxygen species responsible for the effect", *J. Photochem. Photobiol. A Chem.* **106**, 51–56.
[5] Sunada, K., Kikuchi, Y., Hashimoto, K. and Fujishima, A. (1998) "Bactericidal and detoxification effects of TiO_2 thin film photocatalysts", *Environ. Sci. Technol.* **32**, 726–728.
[6] Kim, B., Kim, D., Cho, D. and Cho, S. (2003) "Bactericidal effect of TiO_2 photocatalyst on selected food-borne pathogenic bacteria", *Chemosphere* **52**, 277–281.
[7] Gai, R., Hashimoto, K., Itoh, K., Kubota, Y. and Fujishima, A. (1991) "Photokilling of malignant cells with ultrafine TiO_2 powder", *Bull. Chem. Soc. Jpn.* **64**, 1268–1273.
[8] Cai, R., Hashimoto, K., Kubota, Y. and Fujishima, A. (1992) "Increment of photocatalytic killing of cancer cells using TiO_2 with the aid of superoxide dismutase", *Chem. Lett.*, 427–430.
[9] Sakai, H., Baba, R., Hashimoto, K., Kubota, Y. and Fujishima, A. (1995) "Selective killing of a single cancerous T24 cell with TiO_2 semiconducting microelectrode under irradiation", *Chem. Lett.*, 185–186.
[10] Gai, R., Kubota, Y., Shuin, T., Sakai, H., Hashimoto, K. and Fujishima, A. (1992) "Induction of cytotoxicity by photo-excited TiO_2 particles", *Cancer Res.* **52**, 2346–2348.
[11] Ackroyd, R., Kelty, C., Brown, N. and Reed, M. (2001) "The history of photodetection and photodynamic therapy", *Photochem. Photobiol.* **74**, 656–669.
[12] Wamer, W.G., Yin, J.J. and Wei, R.R. (1997) "Oxidative damage to nucleic acids photosensitized by titanium dioxide", *Free Radic. Biol. Med.* **23**, 851–858.
[13] Saito, T., Iwase, T., Horie, J. and Morioka, T. (1992) "Mode of photocatalytic bactericidal action of powdered semiconductor TiO_2 on mutans streptococci", *J. Photochem. Photobiol. B* **14**, 369–379.
[14] Dunford, R., Salinaro, A., Cai, L., Serpone, N., Horikoshi, S., Hidaka, H. and Knowland, J. (1997) "Chemical oxidation and DNA damage catalysed by inorganic sunscreen ingredients", *FEBS Lett.* **418**, 87–90.
[15] Nakagawa, Y., Wakuri, S., Sakamoto, K. and Tanaka, N. (1997) "The photogenotoxicity of titanium dioxide particles", *Mutat. Res.* **394**, 125–132.
[16] Kashige, N., Kakita, Y., Nakashima, Y., Miake, F. and Watanabe, K. (2001) "Mechanism of the photocatalytic inactivation of Lactobacillus casei phage PL-1 by titania thin film", *Curr. Microbiol.* **42**, 184–189.
[17] Chumakov, P. (1990) *EMBL Data Library*, accession number X54156.